Journal of Thermal Analysis and Calorimetry (2023) 148:13729–13760
https://doi.org/10.1007/s10973-023-12602-6

Hydrothermal performance through multiple shapes of microchannels (MCHS) using nanofluids: an exhaustive review

Nehad Abid Allah Hamza[1] · **Isam Mejbel Abed**[2]

Received: 10 June 2023 / Accepted: 16 September 2023 / Published online: 13 November 2023

Abstract

Hydrothermal performance through multiple shapes of microchannels (MCHS) using nanofluids is summarized as the previous studies in the present work. The enhancement of heat transfer dissipation in electronic equipment becomes more necessary where high heat can damage it and cause more problems, so the Microchannel heat sinks can be a solution fore these problems. The heat transfer enhancement through Microchannels can be acheived by a passive technique which includes using corrugated channels such as wavy, zigzag, and converge-diverge MCHS. Also, flow disruptions such as using MCHS with cavities, ribs, grooves, dimples, and offset strip pin fins. In otherside the fluid additives included using nanofluid with different MCHS shapes, and Secondary flow as an MCHS with oblique fins is another method fore passive techniques. Wavy microchannels with secondary channels have higher hydrothermal performance compared to other types. Zigzag MCHS could provide good heat transfer enhancement but with high pressure drops. Regarding flow disruptions, the hydrothermal performance of MCHS with ribs is better than pin fin. The results showed that using a hybrid nanofluid gives more enhancement heat transfer as well as higher pressure drops. Concerning single-phase fluid, the review results showed that using metal oxide nanofluid has higher thermal conductivity compared to carbon-based and dielectric nanofluids; therefore, the single phase of nanofluids can be arranged descending from the best to worst, according to its use as the cooling liquid in microchannels and their efficiency in heat transfer enhancement, metals (Ag, Cu), metal oxides (TiO_2–H_2O, CuO–H_2O, ZnO–H_2O, and Al_2O_3–H_2O), and dielectric nanofluid (SiO_2–H_2O). The specific application requirements and design considerations will guide the selection of the appropriate microchannel type for optimal heat transfer performance, so MCHS with mixing flow, higher thermal conductivity nanofluids, and low pressure drop are the most important factors that achieve hydrothermal efficiency.

Keywords Hydrothermal performance · Microchannel · Nanofluids · Multiple shapes · Thermal conductivity

List of symbols

HC	Height of MCHS
C_p	Specific heat
K	Thermal conductivity
T	Temperature
KB	Boltzmann constant
u_p	Brownian velocity of the nanoparticles
Nu	Nusselt number
Re	Reynold number
W_t	Width of the tapered channel
W	Mass
W_C	Width of channel

Abbreviations

AR	Aspect ratio
CNT	Carbon nanotube
CCHS	Crosscutting zigzag flow channel
CCZH	Single crosscutting zigzag flow channel
DC	Divergent–convergent microchannel
EG	Ethylene glycol
GnP	Graphene nanoplatelets
DLMCHS	Double-layer microchannel heat sink
Hs	Substrate thickness
HTP	Heat transfer performance
RMCH	Rectangular microchannel heat sink
RSC	Rectangle with semicircular
SLMCHS	Single-layer microchannel heat sink

✉ Nehad Abid Allah Hamza
nehad.ali@wrec.uoqasim.edu.iq

[1] College of Engineering, Al-Qasim Green University, Hillah 51001 Babylon, Iraq

[2] Mechanical Engineering Department, College of Engineering, University of Babylon, Hillah 51001 Babylon, Iraq

TLMCHS	Triangular layer microchannel heat sink
TWC_L	Transversal wavy channel left
TWC_R	Transversal wavy
Tri.C–C.R	Triangle cavity with circular rib
MCH	Microchannel heat sink
MHSIJD	Microchannel heat sinks with impinging jets
W/EG	Water/ethylene glycol
MWCNT	Multi-wall carbon nanotube
MC-AWTR	All wall trefoil ribs
MC-SWTR	Side wall trefoil ribs
MC-BWTR	Bottom wall trefoil ribs
PVD	Physical vapor deposition
PF	Pin fin
ZSMHS	Zigzag serpentine microchannel heat sink
WMCH	Wavy microchannel heat sink
WMSC	Wavy microchannel with the secondary channel
VG	Vortex generator

Subscripts

b	Bottom wall
bf	Base fluid
c	Channel
nf	Nanofluid
np	Nanoparticle
t	Top wall
s	Substrate
w	Wall

Greek symbols

ρ	Density (kg m^{-3})
μ	Dynamic viscosity [kg $(m\ s)^{-1}$)]

Introduction

In most thermal engineering equipment, the excessive heat generated must be dissipated to keep it for a long time and work with more performance; hence, the microchannel heat sinks appear to be one of the solutions to achieve these demands. Microchannel heat sinks (MCHS) are a class of heat exchangers that contain small channels that have hydraulic diameter smaller or equal to 200 mm to give more enhancement in heat transfer between a fluid and solid surface. So the MCHS are used in various industries where efficient heat dissipation is essential, such as electronic cooling (microprocessors, power amplifiers, and LED arrays) [1], power generation systems such as solar and fuel cells to enhance the performance of energy conversion and maintain optimal operating temperatures of these systems [2], aerospace applications to manage the thermal loads experienced by components in aircraft and spacecraft systems [3], automotive cooling to give efficient cooling and manage higher heat loads for components such as engine control modules, battery systems in electric vehicles, and power electronics in hybrid vehicles [4], medical applications such as laser systems, medical imaging equipment, and diagnostics tools to prevent the overheating and ensure accurate operation [5], heat recovery systems in order to transfer waste heat from industrial processes for other applications, such as space heating or preheating of fluids and in bioengineering, aerospace, micropumps, microturbines, engines, microvalves, and microreactors [6]. So according to the above applications more cooling techniques are being used to reduce heat flux, but more research is still needed to extract heat flux greater than 800 W cm^{-2}. As a result, proper thermal management of microelectronics requires overcoming heat flux-related damages. Because of this, incorporating a reliable cooling system into the design of these devices has become crucial. So, microchannel configurations are one of the crucial techniques capable of dissipating high power densities (more than 1000 W cm^{-2}) as opposed to traditional channels. The systems include a cooling medium (air or liquid) and thermal sinks in different shapes and designs. The rapid development of electronic chips has focused the attention on the flow of fluid and heat transfer researchers leading to improving cooling systems. However, the smooth, straight microchannel heat sinks mentioned above cannot cool electrical components properly; this can be attributed to the constantly increasing power density of high-density microelectronics, optical devices, instrumentation, and other devices. Advanced electronic systems cannot continue to evolve with their current level of heat dissipation. Numerous novel designs have been proposed for improving the heat transfer efficiency of MCHS. These designs include using "a secondary channel" [7, 8], "nanofluids" [9, 10], "a channel with curvatures" [11, 12], "dimples, porous" [13, 14], "ribs" [15–24], "cavities or ribs" [25–31], and "a combination of ribs and grooves" [32–37]. The geometry of the microchannels may not be sufficient to meet the demand for high thermal performance, so more researchers investigated the effect of using the cooling liquid on the hydrothermal performance of microchannels.

The novelty and needs of this work may be summarized as follows:

1. Study the techniques of heat transfer augmentation that can be used in MCHS.
2. A significant number of researchers have independently examined a study of the relationship between microchannel structure, hydrothermal performance, and the thermal properties of nanofluids. Few researchers have looked into how different MCHS shapes can affect the hydrothermal performance of a mixture of flowing

nature, type of nanofluid, volume fraction, percentage of nanofluid, particle size, and MCHS shape.
3. The most mathematical equations and models related to calculating the thermal properties of most nanofluids used as cooling liquids are reviewed.
4. Predictive models that have high hydrothermal performance.

Hydrothermal enhancement in MCHS

Generally, hydrothermal enhancement techniques for any thermal engineering system can be classified into two types which are passive and active techniques. Passive techniques are those that do not require direct application of external power, while active techniques require external power. Figure 1 shows a schematic of methods used for heat transfer augmentation.

Active methods

The passive technique has more attention than the active technique because of its role in enhancing the hydrothermal performance of MCHS due to its compact design of electronic devices. However, few researchers tried to enhance heat transfer performance using the active method. Flow-induced vibration is one method of active technique, Go [38] used this method to show the effect of flow-induced vibration of a microfin array on hydrothermal performance. The study proved that increasing the vibration displacement led to a high heat transfer rate. In another related work, Krishnaveni et al. [39] proposed heat transfer can be enhanced using the periodic electric field technique in rectangular MCHS due to chaotic mixing in a microchannel resulting in heat transfer augmentation. The magnetic field is one method of active techniques, in this field gives a rate of enhancement in heat transfer rate, Selimefendigil et al. [40] proved that the heat transfer factor is enhanced by 13.8% when using a magnetic field with nanofluid through a triangle-shaped cavity.

Hydrothermal enhancement for multiple shapes of MCHS using passive technique

Due to the significance of the passive technique in selecting the best MCHS design, the following methods for hydrothermal performance in MCHS will be reviewed in this paper:

- Developing the fluid flow by optimizing the design of MCHS such as in straight MCHS,
- Channel curvatures (corrugated channels) such as in wavy, zigzag, and converge–diverge MCHS [11, 52–76],
- Flow disruptions such as using MCHS with cavities, ribs, grooves, and offset strip fins, [32, 77–113]
- Fluid additives, such as using nanofluid with different shapes of MCHS [32, 74–172]

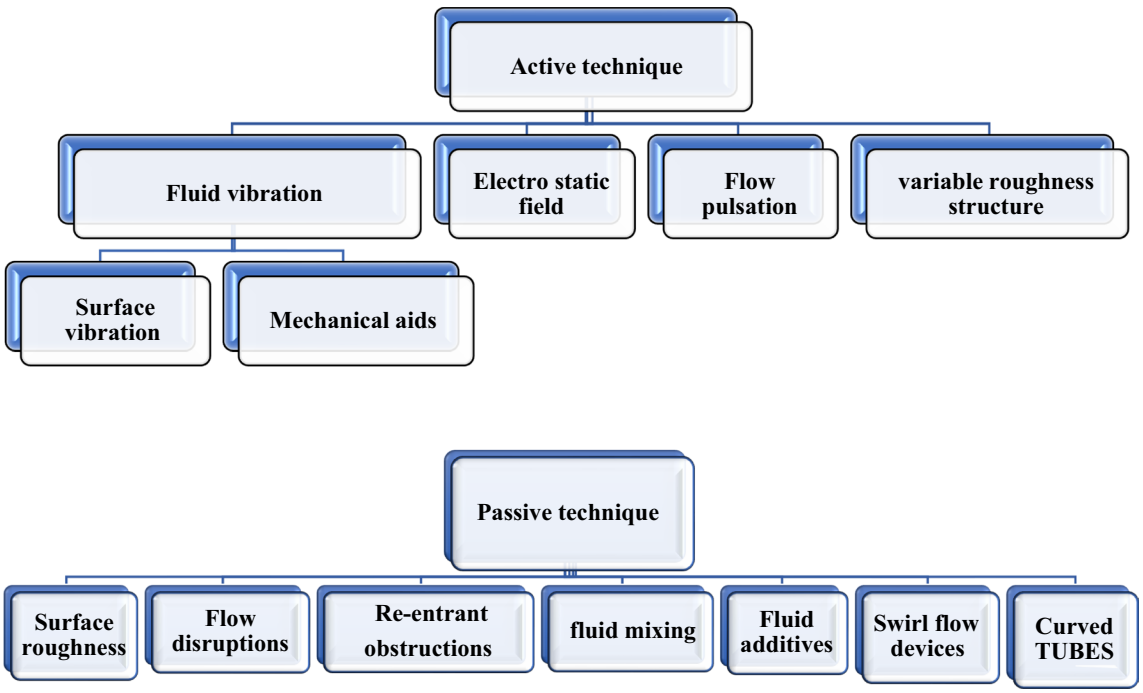

Fig. 1 Different methods of hydrothermal enhancement

- Secondary flow such as in MCHS with oblique fins [59] or microchannel with an alternatively directed slanted secondary channel [61],

Straight microchannels

In the present topic, a passive method for enhancing the performance of MCHS is represented by optimizing the design, single phase (distilled water as a cooling liquid), laminar flow, and 3-D. Heat transfer enhancement can be achieved by breaking the thermal boundary layer and uniformity of temperature distribution with a low pressure drop in fluid flow. The straight MCHS whether single layer or multiple layers have different shapes of cross sections such as rectangular, triangular, and trapezoidal. Wang et al. [41] examined the effect of multiple shapes of MCHS, including rectangular, triangular, and trapezoidal. The findings show that thermal resistance was lowest in the RMCH and highest in trapezoidal. Moreover, the effect of the aspect ratio (AR = Hc/Wc) of RMCH on performance was investigated, where an (AR) between 8.904 and 11.442 resulted in the greatest performance (Fig. 2).

Li and Peterson [42] performed a numerical study on the heat transfer capabilities of silicon-based parallel MCHS.

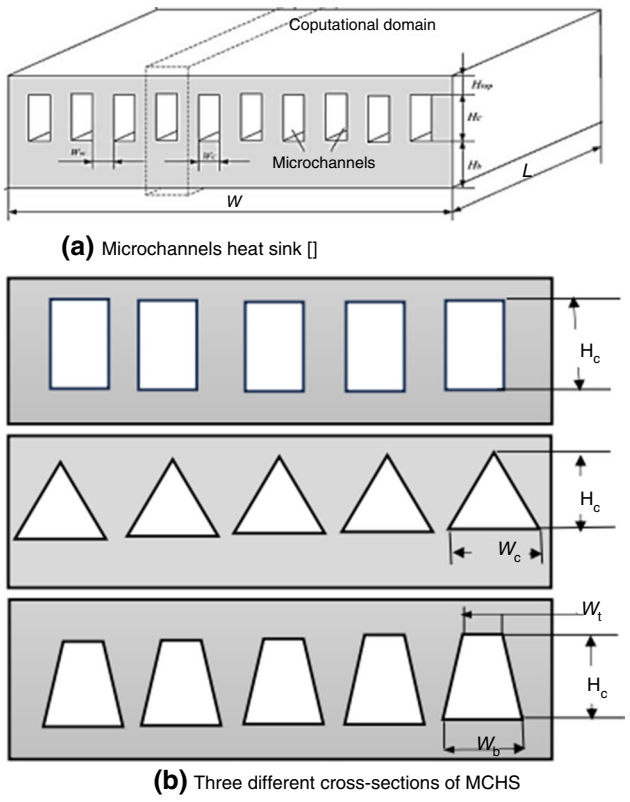

Fig. 2 Schematic of **a** microchannel heat sink geometry and **b** cross section with its dimensions of different microchannels studied by Wang et al. [41]

The optimal geometric properties of the microchannel were verified and indicated there is an increase in the overall cooling capacity exceeding 20% at a pumping power of 2 W and that the thermal resistance was 0.068 C W^{-1}. On the other side, the pressure difference remains constant. Kou et al. [43] Provided a 3D numerical model of the MCHS to examine the effects of heat transfer characteristics caused by different channel heights and widths. The findings demonstrate that lower thermal resistance can be achieved with a bigger flow area, more flow power, and a thinner substrate.

A numerical analysis study by Chein and Chen [44] was used to examine the impact of various inlet and outlet configurations on the thermal behavior of microchannels. The results showed that the velocity and temperature homogeneity of the MCHS, with the supplying of coolant and collection occurring vertically via the flow path from inlet to outlet on the microchannel heat sink cover plate, were very well. Mansoor et al. [45] used Fluent commercial software to analyze the heat transfer performance in a rectangular microchannel by examining the Nusselt number at a range of Re from 500 to 2000. The model was a three-dimensional, laminar flow, and water was used as a cooling liquid. Thermal characteristics in a copper microchannel were investigated using a heat rate per unit area equal to 130 W cm^{-2}. The findings demonstrate that as heat flux continued to increase, the coefficient for heat transfer decreased. Also, the results showed that the $\overline{Nu}$ increased with increasing Re ranging (from 500 to 2000) at heat rate per unit area ranging from 45 and 130 W cm^{-2}.

Shkarah et al. [46] investigated various shapes of rectangular microchannels with widths of 44–56 µm, heights of 287–320 µm, and lengths of 10 mm. Aluminum, silicon, and graphene were used as materials. A fully developed laminar water flow was used at different volumetric flow rates and heat flux values. The results showed that using graphene in the microchannel reduced thermal resistance. The numerical method treated the thermophysical properties of the materials as non-temperature-dependent, which impacted the results compared to the experimental setup, and the findings have yet to be verified experimentally.

The hydrothermal performance of microchannels was examined numerically by Feng et al. [47]. The authors used a wire coil placed at different locations of the microchannels to examine this effect on heat transfer performance as shown in Fig. 3. In the experiment work, distilled water was used as a cooling liquid. The study's findings demonstrated that the longitudinal vortex created by the wire coils effectively improved the MCHS's heat transfer capability, but at the same time, resistance of flow increased. At a heat flux of 400 kW m^{-2}, the MCHS with a long wire coil positioned at the center line of the microchannel exhibits the best heat transfer performance with a performance factor of 1.4–1.8.

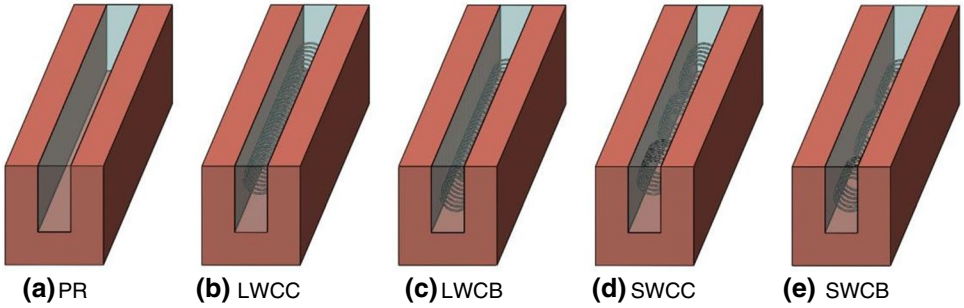

Fig. 3 Different configurations of rectangular microchannels [47]

An algorithm of multi-objectives was used by Yildizeli and Cadirc [48] to optimize the conjugated heat transfer in MCHS. The best trade-off results from maximizing the transfer of pumping power and convective heat, which are mutually exclusive. Microchannel heat sinks with different AR had been optimized for thermal performance and power consumption for Reynolds numbers 13 to 360 using Fluent flow solver and MATLAB optimization. The results revealed that increasing the AR reduced pressure loss and improved thermal performance up to a certain point. Fluid flow type is one method of passive technique that enhances heat transfer and takes attention from researchers. The effect of fluid flow type (parallel and counterflow) in double-layer rectangular MCH has been investigated by Xie et al. [49]. The findings of this work are that the counterflow gives better performance at large flow rates and uniform temperature rise. On the other hand, superior performance is achieved with parallel flow at slightly higher values of flow rates. Conventional DLMCHS design enhances the uniformity of temperature. Findings showed that the temperature of the cooling liquid is high temperature compared to the cooling at the bottom at the inlet region of the bottom channels, resulting in inevitable heating. Leng et al. [50] optimized a unique DLMCH with truncated top channels. The optimization process involved maintaining a constant volumetric flow rate of coolant and a fixed pumping power while experimenting with various design configurations. Employing an alternation structure with the staggered flow with MCHS enhances its overall thermal performance by facilitating the flow switching between the two channels. Shen et al. [51] provided a new structure for parallel and counterflows that include various staggered flow patterns. This structure has led to better temperature uniformity in a DLMCHS. Table 1 shows summary of previous studies related to straight microchannel heat sink.

Corrugated microchannel heat sink

Undoubtedly, one of the key applications in the area of passive heat transfer augmentation techniques is corrugated channels. This method significantly improves the flow mixing between cooler fluid layers in the core region and hotter fluid layers near the channel wall. Dean vortices (DVs) and chaotic advection (CA) are thought to be the mechanisms responsible for the induction of high-flow mixing. It is typical to fully comprehend these mechanisms. Wavy and zigzag are the main shapes of corrugated microchannels; hence, in this part, an exhaustive review will be presented by focusing on the hydrothermal performance of different shapes of the corrugated microchannel and the main parameters that affect performance.

Configurations of Wavy MCHS (WMCHS)

The effectiveness of wavy microchannels in reducing temperature fluctuations in electronic devices was studied numerically by Ghorbani et al. [52]. The proposed wavy MCHS is schematically shown in Fig. 4. Five wavy patterns were taken into consideration, with an amplitude (A) range (62.5 to 250 µm) and wavelength (L) range (1250–5000) µm. The flow regime was laminar, and the heat flux varied at five values: 80, 120, 160, 180, and 240 W cm^{-2}. The outcomes showed that in geometries with larger (A/L) ratios, transverse flow amplification improved heat transfer. A wavy case with a 2500 µm as wavelength and 250 µm amplitude was the ideal geometry. Chips can operate at higher heat fluxes because of the improved heat transfer provided by the use of wavy patterns in heat sinks. The findings from this study are displayed in Fig. 5.

Sui et al. [53] presented a numerical study of heat transfer in 3-D wavy MCHS with rectangular cross sections under study conditions such as constant wall heat flu, constant wall temperature, and conjugate conditions with water laminar flow. In this research it can be noted, the Navier–Stokes equations were solved using FVM based on CFD. The dynamical system technology was used to analyze fluid mixing. According to the simulation results, chaotic advection, which occurs when liquid flows through wavy MCHS, can significantly improve the process of fluid mixing and heat distribution performance while incurring a significantly lower pressure drop penalty than straight-type

Table 1 The literature sources reporting studies related to straight microchannel

Reference	Method and dia. analysis	Case study	Type design	Findings
Li and Peterson [42]	Numerical	To achieve efficient heat in straight MCHS	Rectangular	An increase in overall cooling capacity reached 20% at a pumping power of 2 W and thermal resistance was 0.068 C W^{-1}
Kou et. al [43]	Numerical	To investigate the influence of channel height and width on the heat transfer characteristics	Rectangular	The findings demonstrate that lower thermal resistance can be achieved with a bigger flow area, more flow power, and a thinner substrate
Chein and Chen [44]	Numerical	To investigate the effect of various outlet and inlet configurations on fluid flow and heat transport in microchannel heat sinks	Rectangular with multiple shapes of manifolds	Distributing and collecting coolant vertically will improve heat sink performance
Mansoor et al. [45]	Experimental	To analyze the heat transfer performance in rectangular microchannel by examining Nusselt number at a range of Re from 500 to 2000	Rectangular	The Nu increased with the increasing of ranging (500–2000) at heat flux ranging from 45 and 130 W cm^{-2}
Shkarah et al. [46]	Numerical and Experimental	To study the effect of material used to manufacture microchannel (aluminum, silicon, and graphene)	Rectangular	The results showed that using graphene in the microchannel reduced thermal resistance. However, the findings have yet to be confirmed
Feng et al. [47]	Numerical and Experimental	The effect of the length and arrangement of wire coil inserts on hydrothermal performance	Rectangular	The study's findings showed that the longitudinal vertexing created by the wire coils improved the HTP
Xie et al. [49]	Numerical	The effect of fluid flow type (parallel and counterflow)	Double-layer MCHS	The findings of this work are that the counterflow gives better performance
Leng et al. [50]	Numerical	To optimize a unique double-layer microchannel	Double-layer microchannel with truncated walls	The overall performance enhanced by staggered flow alternation structure
Shen et al. [51]	Numerical	To investigate the effect of flow mixing	Double-layer microchannel	Excellent rising pumping power by using a mixed-flow structure

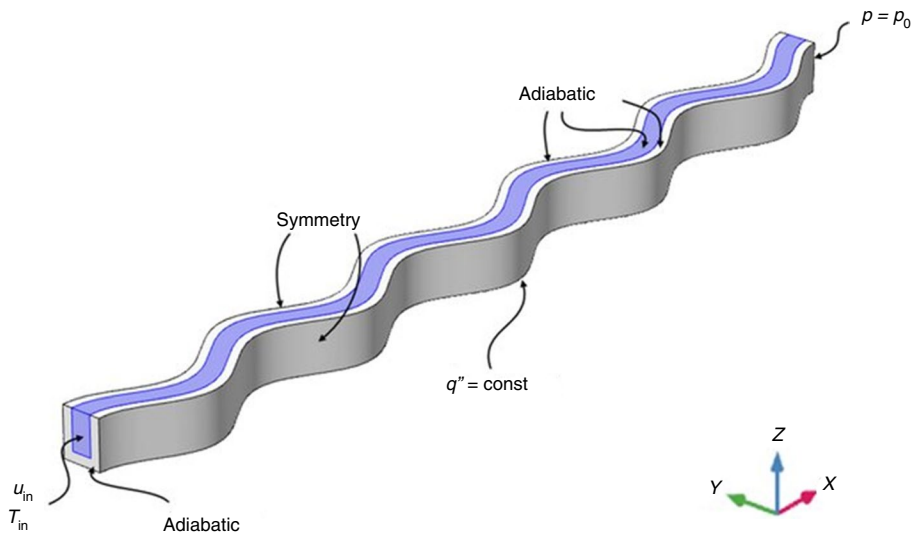

Fig. 4 Schematic of wavy channel and the desired boundary conditions Ghorbani et al. [52]

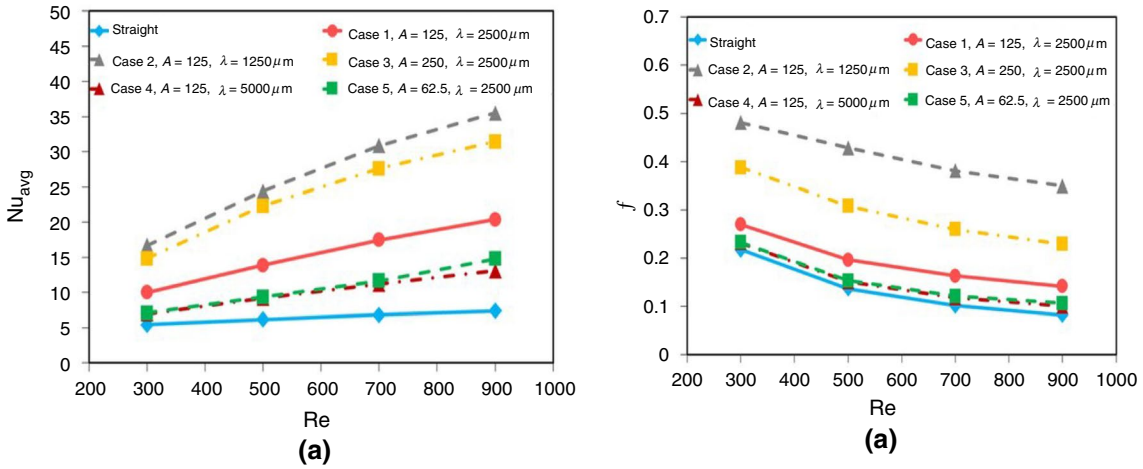

Fig. 5 Comparison for **a** "the average Nusselt number" and **b** "friction factor versus the Reynolds number." Ghorbani et al. [52]

microchannels. Following this study, heat transfer and flow friction were presented.

Sui et al. [54] performed experimentally. The authors study heat transfer in three types of wavy microchannels with rectangular cross sections. The test section has a width and depth of 205 μm and 404 μm, respectively. Different values of wavelength magnitudes (0, 138, and 259 μm) were studied. The number of channels in test section 60–62 wavy (sinusoidal) microchannels distributed in parallel. Reynolds' numbers range from 300 to 800. The researchers made a comparison between the performance in heat transfer between wavy microchannels' and straight microchannels. The results showed that wavy microchannels were more effective than straight microchannels in hydrothermal. Other types of 3D WMCHS heat sinks are raccoon and serpentine wavy MCHS, with rectangular cross sections and Dh of 500 μm studied by Kota et al. [55]. At three different Reynolds numbers (50, 100, and 150), the impact of wavelength, inverse aspect ratio, and amplitude on heat augmentation performance was examined. The heat transfer by the thickness of the thermal boundary layer and in both wavy microchannels was found to be improved by increasing the Reynolds number, wave amplitude, and decreasing the wavelength. Xie et al. [56] proposed a transversely wavy microchannel with a rectangular cross section. The effect of this design on thermal performance has been investigated numerically. The findings demonstrated that compared to a straight microchannel, a transversally wavy microchannel has a significant potential to reduce pressure loss, particularly for higher wave amplitudes at the same Reynolds number. The results showed that the transversal wavy microchannel outperformed the conventional straight, rectangular microchannel in terms of total thermal performance. Figure 6 shows a schematic of transversal wavy microchannels.

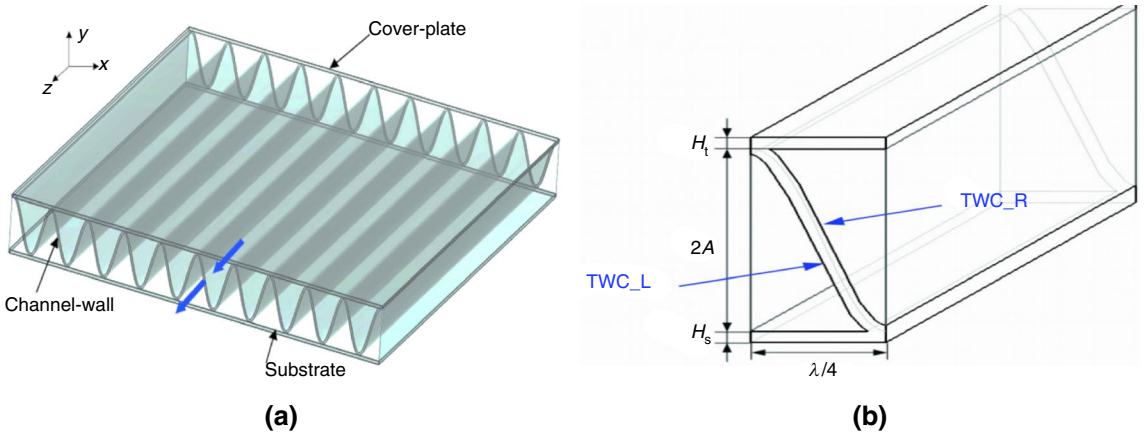

Fig. 6 **a** Transversal wavy microchannels, **b** single transversal wavy microchannel. Xie et al. [56]

A developed flow with heat transfer in rectangular cross section with periodic converging–diverging channels was investigated by Yong et al. [57]. This study presented three types of study (experimental theoretical and CFD simulations). The conditions of this study are liquid water as a cooling liquid and constant wall temperature conditions. This research demonstrates that the fluid behavior and formulation of recirculating vortices are controlled by the channel aspect ratio (AR), with an AR between 0.5 and 1.0 ideal. Furthermore, it looks into how converging–diverging channels with sinusoidal profiles and continuous curvature can outperform straight microchannels by as much as 60% in thermal–hydraulic efficiency.

Gong et al. [58] compared the three proposed designs of dimpled and undimpled wavy microchannels and a straight microchannel to conclude on their relative merits. Hydrothermal properties in WMCHS with dimples at the base of each microchannel were studied numerically. The findings showed that the hyper method of passive technique (wavy with dimpled) achieved high heat transfer enhancement

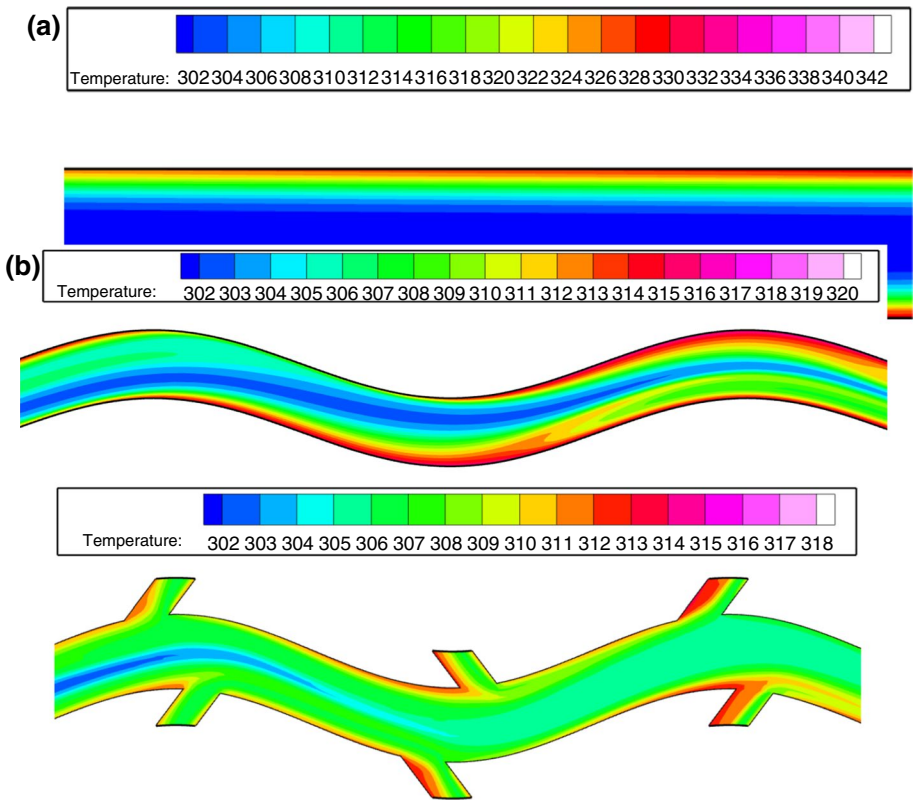

Fig. 7 Contours of temperature distribution **a** RMCHS, **b** WMCHS and **c** WMSC on x–z plane at $y = 0.25$ mm with Re = 600 [59]

compared to straight without dimples and straight with dimples.

Ghani [59] used the combined techniques (secondary flow and channel curvature) depicted in Fig. 7 to improve heat transfer in MCHS. This study investigated the effects of three structural parameters, with amplitudes ranging from 0.05 to 0.2 mm, secondary channel widths from 0.1 to 0.2 mm, and angles of inclination from 45° to 90°. The results were compared to those of WMCHS lacking secondary channels and straight MCHS has same conjugated area. The findings revealed that 0.1 mm amplitude, 0.2 mm secondary width, and a 45° angle of inclination were ideal structural parameters, and thermal performance rose by about 108%.

Kumar et al. [60] investigated thermal and hydraulic performances of MCHS numerically and experimentally with air as a cooling medium. Straight, wavy, and wavy with secondary MCHS are the heat sinks investigated in this work. The main assumptions taken into consideration through the numerical study are 3-D, conduction, and convection as modes of heat transfer, and the flow is a laminar model. With respect to various airflow rates, the Reynolds number ranges from 300 to 1900. The experimental method was used to validate the numerical method. According to the study's findings, the wavy with secondary MCHS performed better in terms of thermal–hydraulic performance than the straight and wavy.

Figure 8 illustrates a model developed by Memon [61] that included parallel and trapezoidal secondary flow channels. In one design, the secondary flow passages were parallel, while in the other, they were regular trapezoidal. The "I-type, C-type, and Z-type" inlet–outlet configurations were used to test these designs. The results were calculated in terms of the temperature on the base plate of the heat sink as well as the velocity and pressure profiles within the flow domain. The results of the study demonstrated that compared to the "C-type and Z-type" configurations, the "I-type" inlet–outlet configuration achieves better flow velocity uniformity. Due to the high fluid distribution that can be achieved in "I-type," this can be considered as the perfect model compared to other types.

Khan et al. [62] Numerically studied the cooling performance of the straight, wavy, and dual-wavy microchannels. Al_2O_3 nanofluids with different volume fraction of 1%, 3%, and 6% was as cooling liquid. The fluid is assumed to be an incompressible fluid, laminar flow. Effect of a secondary flow and thermal performance of WMCHS studied by Memon et al. [63]. This study studied many parameters at different flow rates, such as pressure drop, flow profile, temperature profiles, and Nusselt number. The results have been examined along with related trends and those for the standard design.

An asymmetric wavy, double-layer microchannel with porous fins was a design studied by Wang et al. [64]. The hydrodynamic and thermal characteristics of a three-dimensional fluid–solid conjugate model were computationally analyzed in order to make a comparison between two configurations which are "wavy and porous fin" designs. The results demonstrate that WMCHS can dramatically improve HTP and decrease drop of pressure when using the porous fin design. While the symmetrical layout results in a greater reduction in pressure drop, the parallel configurations produce a greater increase in thermal performance. As a result, the pressure drop penalty for two wavy designs using the porous design is roughly the same. Table 2 shows a summary of previous studies related to WMCHS.

Zigzag MCHS

Previous studies on the zigzag microchannels are summarized in this section due to their importance in many industrial applications, such as cooling electronic systems. The existence of bends along the channel can increase the intensity of the turbulence of the fluid and enhance the mixing of the wall fluid and the main channel to strengthen heat transfer [65–69].

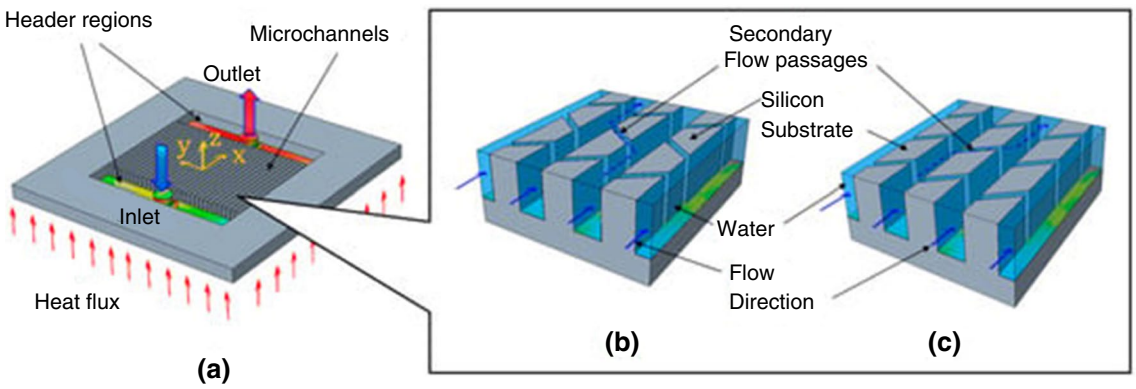

Fig. 8 **a** Sectional view of the MCHS; **b** heat sink with trapezoidal secondary flow (heat sink A); **c** heat sink with parallel secondary flow [61]

Table 2 Summary of previous studies related to wavy MCHS

Researchers	Type of study	Purpose	Remarks/outcomes
Sui et al. [53]	Numerically	To show the effect of amplitude and wavelength on heat transfer and pressure drop	The chaotic advection resulting in a wavy effect, can greatly improve the cooling performance with a much lower pressure drop
Sui et al. [54]	Experimental	to investigate the impact of wavelength on friction and heat transfer and compare the findings with conventional MCHS	Wavy microchannels preferred over straight microchannels
Kota et al. [55]	Numerical	To study the laminar and forced heat for two types of 3D WMCHS	The decreasing of amplitude leads improved heat transfer
Yong [57]	Numerically and Experimentally	To show the effect of aspect ratio on the performance	The optimal channel AR ranges from 0.5 to 1.0. and the converging–divergent wavy was better in cooling and drop of pressure compared to straight MCHS
Gong et al. [58]	Numerically	To examine the characteristic of fluid flow, heat transfer of the different types of wavy microchannels with dimples	Increasing of fluid velocity increase in the local Nusselt number
Kumar et al. [60]	Numerically and experimentally	To study the thermal and hydraulic performances of MCHS	Results show the branched wavy MCHS outperformed the straight and wavy in terms of thermal–hydraulic performance
Khan et al.[62]	Numerically	Make a comparison between three models (wavy, double wavy, and straight MCHS)	It is observed that wavy and dual-wavy channels have high hydrothermal performance compared to straight MCHS
Wang et al. [64]	Numerically	Compare the designs of solid and porous fin wavy configurations	MCHS with a porous fin greatly improve heat transfer performance. Wavy MCHS decrease pressure drop

Mohammed et al. [70] investigated the HTP of MCHS in three different microchannel shapes, namely zigzag, curvy, and step MCHS. The cooling liquid was water in a laminar flow. The outcomes showed that while the temperature was smaller in the ZMCHS, the coefficient of heat transfer was greater. Results also showed that ZMCHS, followed by step and curvy MCHS, could be used to produce high pressure drops. Zheng et al. [71] investigated the hydrothermal characteristics of ZMCHS with cross sections as semicircle under steady-state laminar conditions. Re number ranges from 50 to 320, while the Prandtl number ranges from 0.7 to 20. According to the findings, a lower value for the half-unit length-to-diameter ratio (L/D) results in greater fluctuation in the thermal enhancement factor while simultaneously lowering the drop of pressure. The results also show that the rate that which heat is transferred and drop of pressure rise when the ratio of the radius of curvature to the diameter (Rc/D) is reduced.

Ma et al. [11] introduced a novel offset zigzag microchannel heat sink with 30 parallel channels and basic structural dimensions of 0.1 mm in width, 0.3 mm in depth, 5 mm in length, and 0.2 mm in pitch. The surface's maximum temperature decreases by 5.65 K, and the power of pumping is reduced by 1.4%. At a power of pumping equal to 0.167 W, R_t was also lowered by 17.4%. Because the porosity of the zigzag microchannel reduces the average fluid velocity, it was designed to improve heat transfer and lower flow resistance. [72].

Duangthongsuk [73] compares the thermal behavior of nanofluid flows in crosscutting zigzag heat sinks (CZHS) and crosscutting single zigzag flow channels "CCZHS." SiO_2–H_2O nanofluid with 0.3, 0.6, and 0.8 vol% is used as a cooling liquid. "CZHS and CCZHS" are both made of copper. According to the experimental results, the thermal performance of the nanofluid as a cooling liquid with a heat sink was 3–15% better than that of the water-cooled heat sink. Findings showed that the heat transfer performances of the CCZHS were superior to CZHS by a margin of between 2 and 6% on average.

To increase heat transfer performance Tang et al. [74] constructed a unique heat sink that comprises a zigzag microchannel and a serpentine channel. Also, it incorporated a manifold channel as the input channel to improve flow uniformity. Alnaqi et al. [75] Studied hydrothermal performance in (MCHS) with a zigzag shape under constant heat flux. The MCHS is cooled using hybrid nanofluids (HNFs) nanofluid compounds from "MWCNT/SiO_2/EG-H_2O." Ongoing research investigates the effect of Hybrid nanofluids' velocity (1–2 m s^{-1}), HNF volume fraction (0–0.5 vol%), and zigzag height (0 to 10 mm) on hydrothermal performance. As a result of the increases in velocity, the results showed that a greater amount of heat was removed from the microchannel. In addition,

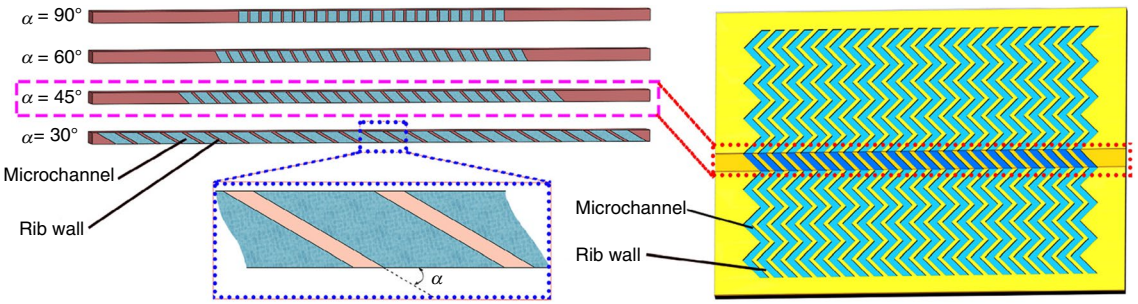

Fig. 9 Incidence angle of the ZSMHS. Peng et al. [76]

expanding the length of the channel's zigzag pattern helps improve heat transfer from the surface of the MHS, which is associated with an increase in the pressure of the fluid moving through the channel. Peng et al. [76] Conducted experiments on a new model with a zigzag serpentine microchannel heat sink (ZSMHS) shown in Fig. 9. The performance of the structure's heat transfer is examined using a zigzag microchannel with four different angles (300, 450, 600, and 900). Investigations were conducted on a number of variables, including pumping power, friction factor, pressure drop, heat transfer coefficient, thermal resistance, and temperature uniformity. The results showed that an angle of 300 could produce the lowest pressure drops, friction coefficients, and thermal resistance of the ZSMHS (Table 3).

Flow disruptions

It was one method of passive technique for heat transfer augmentation in MCHS by using MCHS with ribs, pin fin, dimples, obstacles, and curvature. The heat transfer enhancement can be achieved by interrupting of thermal boundary layer and creating vortices [77]. In the present topic, some of the studies related to flow were disruption studied.

Ribs in MCHS

Unfortunately, high-flow disturbances and the locking flow effect can significantly increase of drop in pressure when ribs are used [78, 79]. As a result, optimizing the geometric characteristics of the ribs is typically required to enhance the cooling of equipment while lowering ΔP. Utilizing MCHS with ribs, grooves, or cavities to interrupt thermal boundary layers and reduce pressure drop is another frequently used method to improve heat transfer [80, 81]. Greater mixing between the hot water that is closest to the walls and the central flow of cold water is made possible by the jet and the throttling structure [27].

A combination of ribs and grooves or cavities effectively improves heat transfer while minimizing pressure drop and taking advantage of the lower pressure drop of grooves or cavities [32].

Ahmad et al. [82] numerically investigated the effect of rib surface refinements on the hydrothermal performance of MCHS. The pressure drop was reduced by as much as 85% and the Nusselt number was reduced by as much as 25% due to the ribs' surface refinement, leading to a thermal enhancement factor of 80%. The effectiveness of both the length and width of the ribs on the hydrothermal performance at different Reynolds numbers was examined by Paramanandam [83]. The main assumption in that study was water used as a cooling liquid with laminar flow and three-dimensional. The effectiveness of MCHS with ribs was measured by performance factor. Results indicate that the effect of rib width is higher in enhancing the heat transfer when compared with its length but with a penalty on the dropping in pressure.

Zhang et al. [84] investigated the thermal performance of MCHS with new trefoil-shaped ribs. This study looked at three trefoil-shaped rib configurations: MC-AWTR, MC-SWTR, and MC-BWTR. At Re = 100–1000, the HTP, Rt, and entropy generation are used to measure the performance of MCHS. The results indicate that adding trefoil ribs to the walls of a smooth microchannel makes it better at handling heat, but it makes it worse at handling pressure. As the Reynolds number gets higher, it also affects the Nu and the $\bar{h}$. The efficient MCHS can be impacted by varying cross sections, and as a result, ribbed microchannel architectures have been developed. The ribs will disrupt the flow boundary layer and the thermal boundary layer, improving heat transmission. Figure 10a–c show different configurations of ribs and cavities. The most recent research on the effects of ribs and cavities on MCHS is compiled in Table 4.

Pin fin MCHS

Later the design of the heat sink was a plate fin heat sink (PFHS), and the air was used as a cooling liquid. This design was considered one of the most traditional designs because of its ease of fabrication. Much research into PFHSs has

Table 3 Summary of previous studies related to zigzag microchannel heat sink

Researchers	Type of study	Purpose	Remarks/outcomes
Mohammed et al. [70]	Numerically	To stat the effect of geometry on the thermal performance zigzag, wavy, and step MCHS have studied	ZMCHS is found to be the best for temperature and heat transfer coefficient. Additionally, the results showed that a high pressure drop in ZMCHS followed by wavy, curvy, and step microchannels
Zheng et al. [71]	Numerically	To Study the effect of Aspect ratio on hydrothermal performance	Decreasing the values of Lz/d and Rc/d causes more fluctuation in the heat transfer enhancement factor, implying an increase in pressure drop
Ma et al. [70]	Numerically	To show effecting of porosity on the heat transfer coefficient	The results indicate with decreasing the porosity the convection heat coefficient increases
Duangthongsuk [73]	Experimentally	To compare the thermal performance of two different types (MCHS) with different zigzag flow channel structures	The findings showed that enhancing in thermal properties of the CCZHS more than those of the CZHS by 2–6%
Alnaqi et al. [75]	Numerical	The purpose of this research is to examine the heat transfer and pressure drop in a microheat sink (MCHS) with zigzag microchannels under constant heat flux	The MHS's ability to dissipate heat is increased as the velocity rises. On the other hand, improving the length of the channel's zigzag helps with heat augmentation from the MHS's surface

gone into optimizing the fins' height, thickness, and separation, with the results being heated transfer predictions. Siuho et al. [88] studied a heat exchanger with staggered square pin fins to show that the heat transfer coefficient is highest close to the inlet and decreases along the flow direction. Liu et al. [89] carried out a test on a microsquare pin fin heat sink with pins in different places. It has been seen that as Reynold's number goes up, both pressure and average Nusselt go down. Three models of pin fins heat sink were studied numerically by Sajedi et al. [90] shown in Fig. 11. The models were circular pin fin heat sink (PFHS), circular pin fin with splitter, square pin fins, and square pin fin with splitter. According to the results, a circular pin fin heat sink with a splitter reduces pressure drop by 13.4%, thermal resistance by 36.8%, and profit factor by 20%. The same results are observed for square pins, with an 8.5% reduction in pressure drop, a 23.8% reduction in thermal resistance, and a 14% increase in profit factor.

Yadav et al. [91] Three ways were used to put some cylinder-shaped microfins in a rectangular microchannel. The upstream finned microchannel worked best at a low Reynolds number (Re). At a high Re, the whole microchannel with fins worked best. The venting holes in the microchannel heat sink described by Yu et al. [92] make separating and removing fluids from the Piranha pin fins easier. Also, the Piranha pin fins disrupt the flow field. This causes the air to distribute, which makes the heat transfer better. Yang et al. [93] examined the heat transfer enhancement with five different configurations of microchannel heat sinks, including pin fin. The cross-sectional geometries of the pin fin have been chosen as circle, triangle, square, pentagon, and hexagon. The overall dimensions of all MCHS were designed to be the same, and a constant heat rate per unit area was applied at the bottom surface of the microchannel heat sink. Similar trends were observed in both the results and the simulations. To maximize the cooling efficiency of single-phase array microchannel heat sinks, the shape of the pin fin was critical in balancing pressure drop and heat transfer rate. The effect of geometry and the working fluid in laminar flow on heat transfer and flow characteristics was examined by Al-Asadi et al. [94]. The first is a heat sink with holes and pins (PPHS). The second is a new design for a uniform microchannel with vortex generators (VGs) of various shapes spaced out along the channel base. The constant volume flow rate of fluid is used to compare the triangle, circle, and rectangle VG shapes. The results show that using water to move heat in PPFHS does not make a big difference. It is also found that of the shapes suggested, circular VGs perform best when it comes to heat.

An experimental study for improving the hydrothermal efficiency of the inclusive MCHS was proposed by Wang et al. [95]. The researchers conducted a new design consisting from PF and VG. The finding showed that fins as a

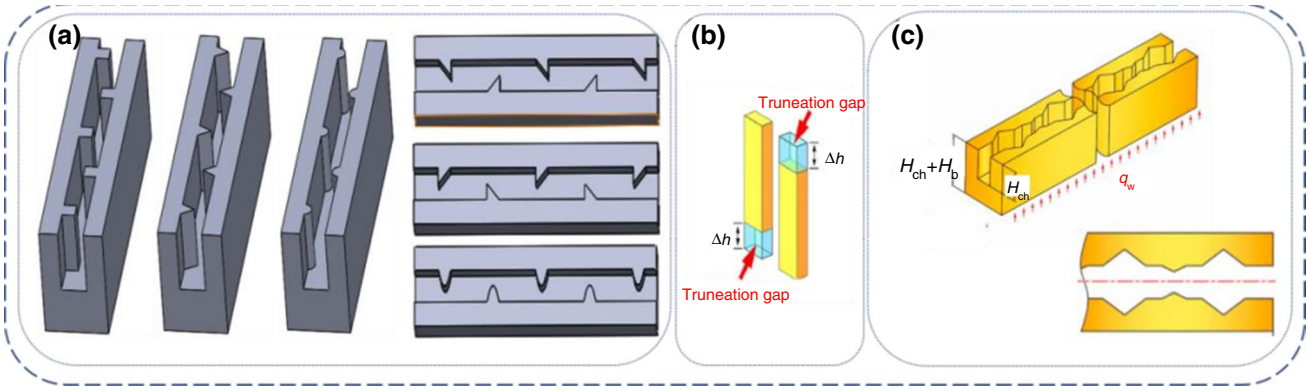

Fig. 10 Different shapes of ribs and cavities: **a** shape of ribs [85]; **b** shape of truncated ribs [86]; **c** structure of cavities and ribs [87]

Table 4 Selected studies related to the microchannel heat sink with ribs

Researchers	Type of study	Purpose	Remarks/Outcomes
Ahmad et al. [82]	Numerical	To show the effect of ribs on hydrothermal performance	In all cases, the surface refinement of the ribs has led to a maximum reduction of 85% in pressure drop, a maximum reduction of 25% in the Nusselt number, and a maximum thermal enhancement factor of 80%
Paramananda [83]		To study the effect of rib dimensions on HTP	Results indicate that the effect of rib width is higher in enhancing the heat transfer when compared with its length but with a penalty on the dropping of pressure
Zhang et al.[84]		The purpose of this study is to analyze the HTP behavior of MCHS featuring novel trefoil-shaped ribs	The Nusselt number and average heat transfer coefficient tend to increase as the Reynolds number increases

pin and vortex generators on MCHS make it easier for the water flow to be disturbed and for efficient heat transfer. This structure is shown in Fig. 12. The results show that oval pin fins perform better than round and diamond pin fins when it comes to thermal and hydraulic performance. When considering Reynolds numbers between 340 and 640, the oval pin fin achieves the best overall performance factor with (0.4 mm) as spacing and (0.1 mm) as height, as shown in the Fig. 13. The vortices will increase the mixing operation of hot fluid cold fluid.

The local coefficient of heat transfer coefficient around a single pin fin in a microchannel was predicted by Wang et al. [96], to maximize the wake's trailing edge downstream of the pin fin. Comparing the heat transfer rates of open and closed heat sinks, Prajapati [97] found that heat sinks with a fin height of 75% to 80% were more efficient than those with a full height of fins. The author has also listed the other benefits of the open microchannel heat sink. The open-type microchannels were investigated experimentally by Kadam et al. [98]. This research focused on improving the heat transfer efficiency of a microchannel heat sink with single-phase flow. A plain MCHS and an extended MCHS configuration of the open type were built. The work studied at mass flow rate per unit area range (157–754 kg m^{-2} s^{-1}) and an effective heat per unit area range (6.1–246 kW m^{-2}). The maximum decrease in wall temperature was measured equal to 3.7 °C. According to the study's findings, fins in the plain open MCHS accelerate heat transfer performance by 15%. Bhandari and Prajapati [99], examined open microchannel configurations with a gap between the fin's top surface and the heat sink's top wall. Seven different heat sinks in the 0.5–2.0 mm range with a 0.25 mm increment were compared in this study. According to the prediction results, raising the heat sink's fin height will speed up heat transfer. Figure 14 show all models are analyzed.

Bhandari and Prajapati [99] validated the average Nu with varying Reynolds numbers for the different values of heat fluxes, where this validation showed that the value of Nu was approximately 10–12% with the prediction relations of Shah and London [100]. Figure 15b proved that the pressure drop predicted by the Bhandari and Prajapati [99] model is in close agreement with the experimental findings of Qu and Mudawar [101].

Pandey [102] presented the results of an experimental investigation into the efficiency of copper pin–fin heat sinks, and parallel microchannel heat sinks using DI water as a

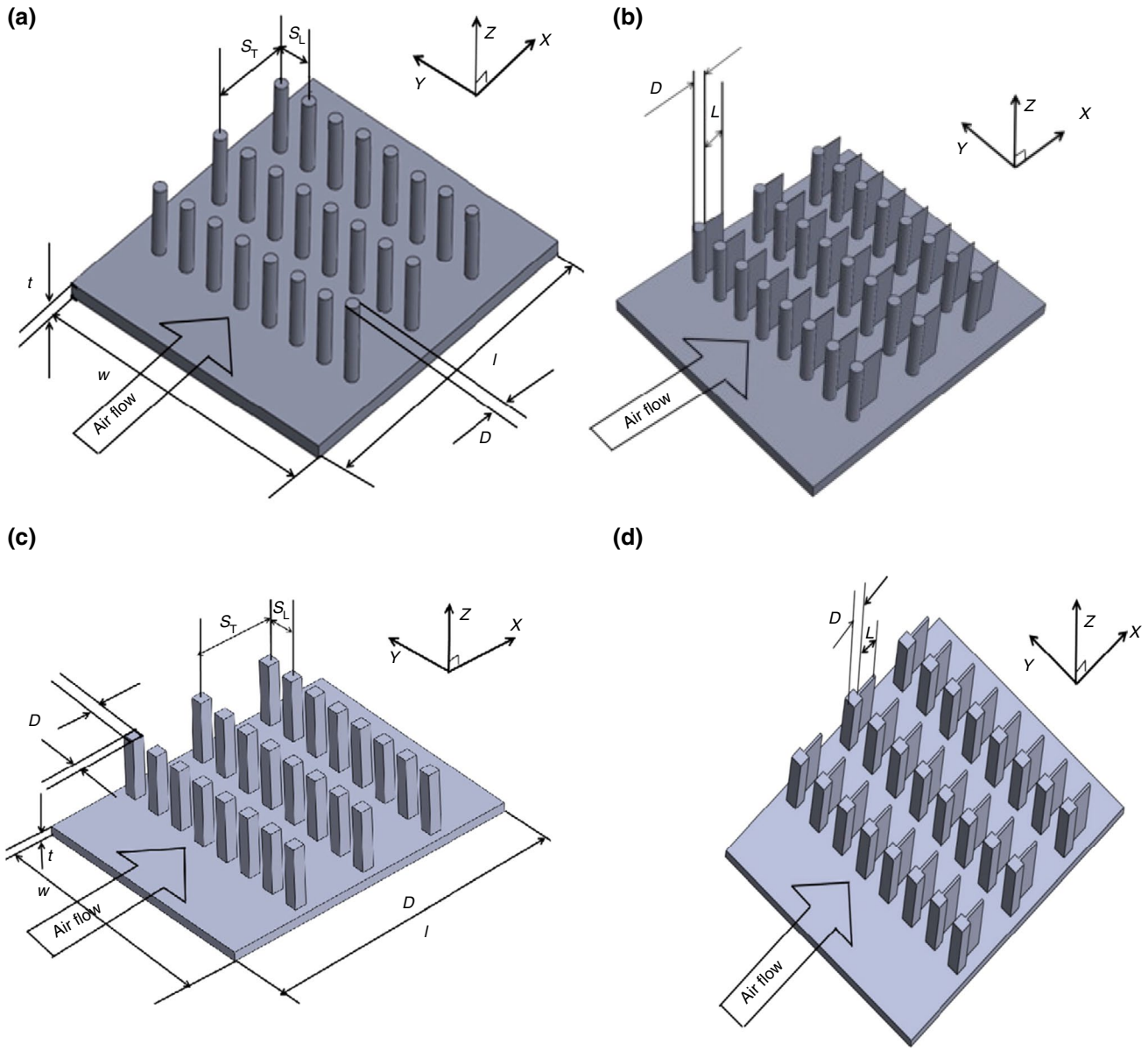

Fig. 11 Configurations of pin fin heat sink **a** circular pin fin **b** circular PFHS with a splitter **c** rectangular PFHS **d** rectangular PFHS with a splitter. Sajedi et al. [90]

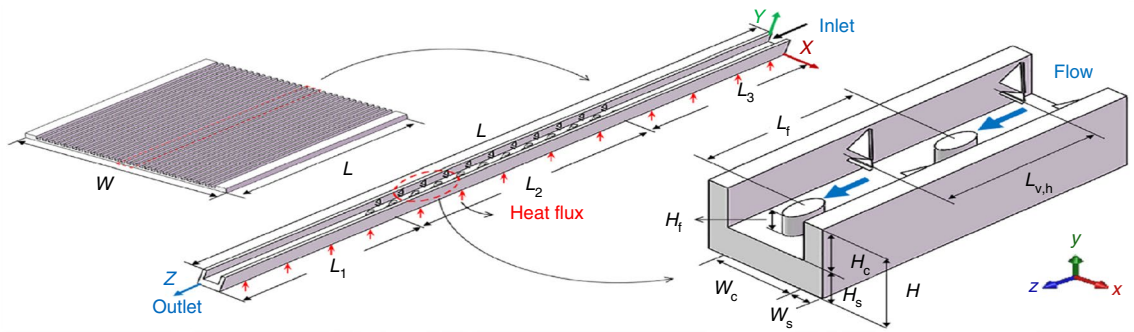

Fig. 12 The schematic diagram of pin fins and vortex generators in the microchannel heat sink Wang et al. [95]

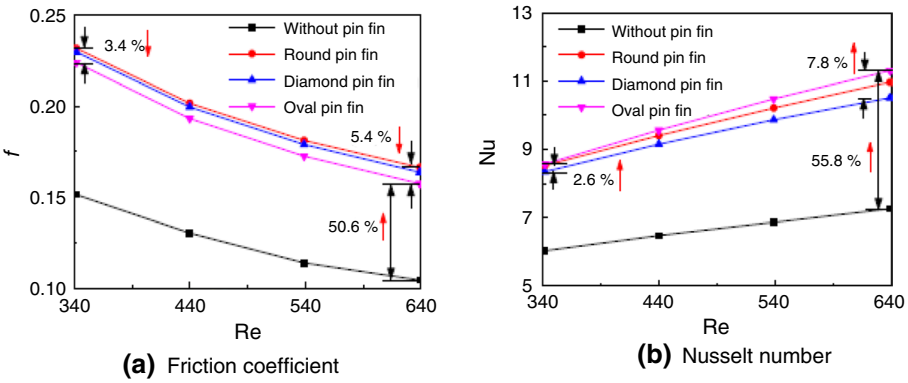

Fig. 13 Variations coefficient of friction and Nu with Re for various cases. Wang et al. [95]

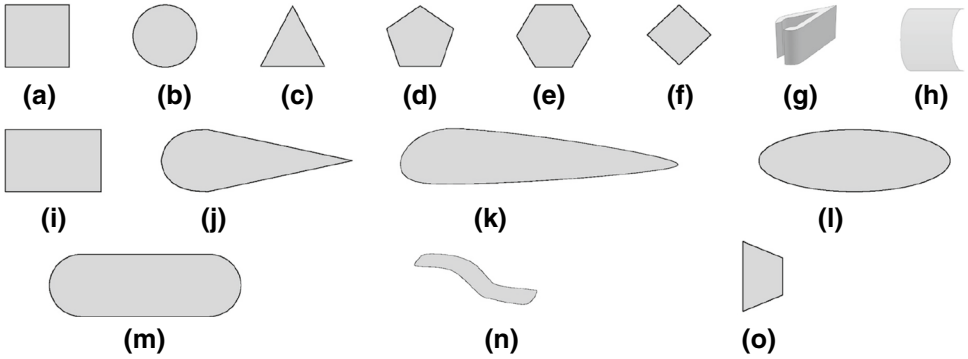

Fig. 14 Sketch of various configurations of pin fin **a** square **b** circular **c** triangular **d** pentagonal **e** hexagonal **f** diamond **g** piranha **h** chevron **i** rectangular **j** cone **k** hydrofoil **l** elliptical **m** oblong **n** S-shaped **o** trapezoidal (Bhandari and Prajapati 2021) [99]

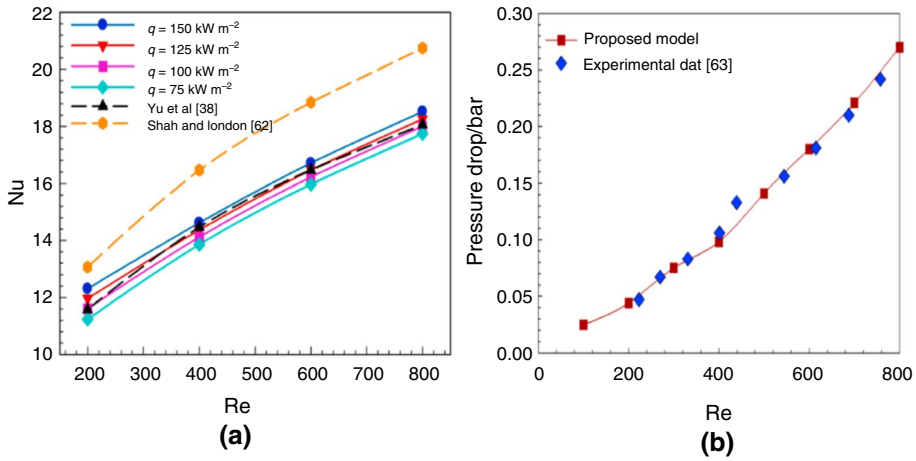

Fig. 15 **a** Comparison of average Nu for a plane channel with the correlations given by Yu et al. [92] and Shah and London [100] **b** Pressure drop validation with Qu and Mudawar [101].

coolant at varying flow rates. Substrate temperature, pressure drop, pumping power, and thermal resistance are among the thermal and hydraulic features examined. The results showed that as pumping power increased, thermal resistance decreased for both heat sinks, albeit at different rates and amounts. Furthermore, increasing the Reynolds number decreased thermal resistance and increased pressure drop for both designs. In the same heat flux conditions, a parallel microchannel heat sink showed lower thermal resistance pumping power than a pin fin heat sink (Tables 5, 6).

Dimples with MCHS

Dimples have been shown in studies [103–105] to increase thermal transmission by disturbing the boundary layer. Microchannel heat sinks using nanofluid [106]. The efficiency of dimples in improving cooling performance was analyzed by Xu et al. [107]. Hydrothermal efficiency is computed numerically for a laminar flow with a Re equal to 500. Due to the dimple effect, the author has found that transverse convection improves convection heat transfer under laminar flow without significantly increasing pressure drop. Because

Table 5 Selected studies related to pin fins MCHS

Reference	Method	Case study	Re range	Working fluid	Findings
Siuho et al. [88]	Experimentally	To examine the heat transfer properties of a single-phase micropin–fin	96–643	deionized water	Local average heat coefficient (h) and Nusselt increase with increasing Reynolds number. The heat transfer coefficient has a higher value near the heat sink inlet and decreases along the flow direction
Liu et al. [89]	Experimentally	To show the thermal performance of square pin fin MCHS	60–800	deionized water	The experimental results revealed that as the Reynolds number increased, the pressure drop and average Nusselt number also increased
Sajedi et al. [90]	Numerically	studying the effect of splitter on the hydro-thermal behavior of a pin fin heat sink	800	deionized water	Results revealed that using a splitter enhances the hydrothermal performance of both circular and square pins, with the largest enhancement occurring when $O = 10\ W$ and $V = 4.5\ \mathrm{m\ s^{-1}}$
Yadav et al. [91]	Numerically	The purpose of this demonstration is to present how an extended surface can be used to improve heat transfer in a microchannel	200–1400	deionized water	Optimization of extended surface microchannel carried successively for several fins, diameter, pitch, and height of fins. There is a 160% enhancement in the average coefficient of convection heat with an acceptable pressure drop penalty
Yu et al. [92]	Experimental and numerical study	To show the hydrothermal performance of Pin Fin (PPF) microchannel heat sinks	508–2114	deionized water	The pressure drop and average surface temperature that was determined by experiments and models were in good agreement. However, the friction factor is higher than in a simple channel
Al-Asadi et al. [94]	Numerically	The effect of geometry and working fluid in laminar flow on heat transfer and flow characteristics	300–2000	deionized water	The findings indicate that there is no significant improvement in heat transfer using water in PPFHS. However, the VGs described here show significant promise in overcoming heat transfer challenges
Wang et al. [95]	Numerically	Effects of pin fins and vortex generators on thermal performance	340–640	Al_2O_3 nanofluids	Using a vortex generator can enhance the HTP by 30%
Wang et al. [96]	Numerically experimentally	To demonstrate thermal performance in three different flow regimes (laminar flow with steady wake, laminar flow with unsteady wake, and turbulent flow),	88–854	deionized water	At the edge trailing of the wake downstream of the pin fin, the local temperature along the centerline was always lower (indicating a higher local heat transfer coefficient) than off the centerline due to vortex shedding and large-scale flow mixing
Bhandari and Prajapati [101]	Numerically	To show the effect of various configurations of pin fin on hydrothermal performance	1100–800	deionized water	It noted that the increasing height of the fin in the heat sink; affects heat augmentation
Pandey [102]	Experimentally	Examination of the performance of parallel microchannel and pin–fin heat sinks made from copper	200–1000		The results showed that increasing the pumping power reduces thermal resistance for both heat sinks at different flow rates

the difference in flow behavior and pressure drop between a standard microchannel and one with dimples is small, the pressure drop is disregarded as negligible when discussing the impact of dimples on heat transfer. Li et al. [108] demonstrated that the depth of dimple and protrusion significantly impacted thermal performance, with the relative Nusselt number Nu/Nuo increasing with flow rate and depth of dimple/protrusion. Huang et al. [109] conducted a numerical study to determine how dimples affect the heat transfer performance of a microchannel heat sink with impinging jets. The authors utilize numerical simulation and the field synergy principle to examine the performance of MIJs with and without dimples of varying dimple structures, including convex, concave, and mixed dimples. Results indicate that IMJS with convex dimples exhibited the best cooling performance, followed by those without mixed and concave dimples. Gan et al. [110] suggested a new model with side outlets for microchannel heat sinks with impinging jets and dimples (MHSIJD). The performance of the MHSIJD with side outlets was studied using a simulation method based on CFD with an RNG *k–e* turbulence model. The analysis indicates that the MHSIJD with side outlets works better at transferring heat. Up to 17.51% more heat transfer capacity is possible. The MHSIJD with side outlets has a lower pressure drop, which can be reduced by nearly 22.39%. The MHSIJD with side outlets also performs better because it cools better and uses less pump power.

The effects of dimples, dimple positions, and dimple sizes on experimental heat transfer and flow friction were studied by Gupta et al. [111]. More heat is dissipated when the dimple diameter is larger. A larger dimpled heat sink with a staggered dimple pattern results in a higher Nu and a higher friction factor. Okab et al. [112] investigated numerically a new design to improve heat transfer. The new design features two dimple sizes (0.5 mm and 1 mm) that are systematically clustered along channels with and without filets at Re numbers ranging from 200 to 1200. Furthermore, the filet profile influences MCHS thermal performance without increasing the pressure drop penalty. The results showed that the construction of dimples with filet profiles significantly enhanced HTP. The Nusselt number of microchannel heat sinks with a 1 mm dimple size, and filet profile is 60% higher than a plain microchannel. A numerical study was conducted by Debbarma et al. [113]. The incorporation of dimples and protrusions improved the double-layer sink's overall performance. Utilizing double layers in the heat sink allows us to get around the problem of the extreme temperature difference. Research into deionized water as a coolant is conducted for the Re ranging from 89 to 924. The results show that dimples or protrusions, regardless of their number or positional pattern, always contribute to an increase in Nusselt number, indicating a higher heat release rate.

Nanofluid synthesis and characterization

Nanofluids can be defined as colloidal suspensions from nanoparticles in a base fluid (water, Ethylene glycol, oil, etc.). Thermophysical properties of conventional fluid improve dramatically when the incorporation of nanoparticles is done. These properties are represented by density, specific heat, thermal conductivity, and dynamic viscosity. The amount of nanoparticles suspended in the base fluid determines the degree of heat transfer enhancement. Metal oxides (Al_2O_3, CuO, TiO_2, ZnO, MgO, SiC, etc.) are preferred as high thermal conductivity nanoparticles. Base fluids that are commonly used are water (H_2O), ethylene glycol (EG), and engine oil (EO) [114]. Various engineering applications utilized nanofluids due to their tremendous potential in improving heat transfer enhancement. From these applications photovoltaic (PV) panels [115]. One promising avenue for their utilization is in microchannels, where the small dimensions present unique challenges and opportunities for enhancing heat dissipation and fluid flow. Research in this area aims to leverage the unique properties of nanofluids to optimize thermal management in microchannel systems, leading to advancements in fields such as electronics cooling, energy systems, and biomedical devices.

Nanofluid preparation

Nanofluids produced by dispersing nanoparticles in the base fluid require good dispersion, which can be improved by using surfactants, surface modification, and strong force. There are two basic methods for preparing nanofluids: one-step physical and two-step physical. Firstly, the percentage of volumetric concentration and the mass of nanofluid must be specific then the mass of nanoparticles determine. The percentage of volume concentration is calculated by Eq. (1). [114]

$$\text{Volume concentration, } \phi = \left[\frac{\frac{W_{sp}}{\rho_{np}}}{\frac{W_{np}}{\rho_{pp}} + \frac{W_{bs}}{\rho_{bs}}} \right] \times 100 \tag{1}$$

where W_{np} denotes the mass of the nanoparticles, W_{bf} is the mass of the base fluid, ρ_{np} is the density of the particle, and ρ_{bf} is the density of the base fluid.

One-step method

This method avoids some procedures, including drying, storing, moving, and dispersing nanoparticles. Physical vapor deposition (PVD) is used to create stable nanofluid. (PVD) technique in which the base fluid is used to carry out direct evaporation and condensation of nanoparticles. Pure and consistent nanoparticles are created using this technique. As a result, nanoparticle accumulation is decreased.

Table 6 Selected studies related to microchannels heat sink with dimple-type

Reference	Method	Case study	Re no.	Working fluid	Major finding
Xu et al. [107]	Numerically	The efficiency of dimples in improving cooling performance	500	DI water	Due to the dimple effect, the transverse convection improves convection heat transfer under laminar flow without significantly increasing pressure drop
Li et al. [108]	Numerically	Effects of depth of dimple and protrusion	–	DI water	The thermal performance was largely affected by the depth of dimple and protrusion
Huang et al. [109]	Numerically	The effect of dimples on the HTP of an MCHS with impinging jets	-	DI water	According to the findings, MIJs with convex dimples performed the best in terms of cooling, followed by those without dimples and mixed dimples
Gan et al. [110]	Numerically	Microchannel heat sinks with impinging jets and dimples: a new design with side outlets (MHSIJD)	–	DI water	Heat transfer is improved in the MHSIJD with side outlets, according to the findings. It is possible to increase heat transfer capacity by up to 17.51 percent
Gupta et al.[111]	Experimentally	The effects of dimples, dimple positions, and dimple sizes on experimental heat transfer	–	DI water	A larger dimpled heat sink with a staggered dimple pattern has a higher Nu and friction factor
Okab et al. [112] investigated	Numerically	The new design considers two dimple sizes (0.5 mm and 1 mm) systematically clustered along the channels with and without filets	200–1200	DI water	According to the predicted results, increasing the height of the fin heat sink increases the HTP
Debbarma et al. [113]	Numerically	Using dimples and protrusion in such a double-layer sink enhanced overall performance	889–924	DI water	Regardless of number and positional pattern, dimple or protrusion always improves Nusselt number, indicating higher heat release

Two-step method

In the two-step method, the nanoparticles are produced using various techniques, and they are then mixed with the base liquid to create the desired nanofluid. This manufacturing procedure costs little and enormous. The two-step method's main flaw is the clumping together of nanoparticles. The use of surfactant is due to instability.

Analyzing the stability of nanofluids

Nanofluid stability is the resistance of nanoparticles against aggregation or sedimentation [116]. There are different methods to examine the stability of nanofluids, such as

- Sedimentation, in this technique the mass or volume of the sediment under external forces must be measured [117]. Sahooli et al. [118] investigated the stability of CuO nanofluid.
- UV–spectrum in this technique the absorbance of light by the nanofluids at different wavelengths must be measured. [116]
- Zeta potential: measuring the electrical charge on the surface of nanoparticles in the nanofluids [114]
- Dynamic light scattering: measuring the size distribution of nanoparticles in the nanofluids [114]

Mathematical relations of properties of nanofluids

Density of nanofluid

The classical mixture law is the formula most frequently used to calculate density. The density of a nanofluid can be described using the classical mixture law as,

$$\rho_{\mathrm{nf}} = \rho_{\mathrm{np}}\phi + (1-\phi)\rho_{\mathrm{bf}} \tag{2}$$

Specific heat of nanofluid

Equation (3) is an expression for the specific heat of nanofluids based on the volume concentration and density of individual element equation [119].

$$\boldsymbol{C_{\mathrm{nf}} = C_{\mathrm{p_p}}\phi + (1-\phi)C_{\mathrm{p_{bf}}}} \tag{3}$$

Zhou et al. [120] showed that Eq. (3) was used for small volume concentration**.** Assuming thermal equilibrium, Xuan and Roetzel [121] proposed Eq. (4)

$$\boldsymbol{C_{\mathrm{p_{nf}}} = \frac{\phi\rho_{\mathrm{np}}C_{\mathrm{p_{np}}} + (1-\phi)\rho_{\mathrm{bf}}C_{\mathrm{p_{bf}}}}{\rho_{\mathrm{nf}}}} \tag{4}$$

Thermal conductivity of nanofluid

Thermal conductivity is the principal property effect on heat transfer enhancement in all thermal engineering systems, so this property can be enhanced by using nanofluid (nanoparticle + suitable fluid). So, choosing appropriate nanoparticle is important. Table 7 demonstrates the thermal conductivity of different nanoparticles.

The following table shows the models used by researchers (Table 8):

Dynamic viscosity of nanofluid

Dynamic viscosity is an important property, the increasing or decreasing of its value effect on the hydrothermal performance of MCHS. When two adjacent layers of fluid moves each to other resistance force will be generated which is namely viscous force that dependent on dynamic viscosity. Theoretically dynamic viscosity considered as a ratio of shear stress to the shear strain rate. Experimentally, dynamic viscosity can be evaluated by using viscometer. So, for its important more than authors take attentions by it and predicted models to calculate the dynamic viscosity. Table 9 show previous literature studies related to calculate the dynamics viscosity.

Using of mono-Nanofluid in MCHS

Hung and Yan [143] studied the effect of using microchannel as a double layer with Al_2O_3 as a nanofluid that increased thermal performance by 26%. The results show that using an Al_2O_3–water nanofluid will result in the greatest improvement in channel cooling, where Al_2O_3 (1%)–water nanofluid shows an average improvement in thermal performance of 26% over that of pure water for a given pumping power. Ahmed et al. [144] numerically investigated the effects of nanoparticle volume fraction on a two-dimensional wavy channel. The Reynolds number and the volume fraction of nanoparticles considered are, respectively, in the ranges of 100–800 and 0–5%. In this work, copper–water nanofluid was used as the working fluid. According to the research, nanoparticles' volume fraction, wavy wall amplitude, and Re were the most important hydrothermal variables. Wang et al. [145] used Al_2O_3 as a coolant liquid in a straight MCHS with a pin fin and vortex generator to increase flow disturbance and mixing flow. A 4% nanofluid with 20 μm Al_2O_3 nanoparticles size provided the best heat transfer. Selimefendigil and Öztop [146] studied numerically effect of pulsating and nanofluid for nanofluids, where pulsating fluid compared to the steady case. The findings show the combined effect of pulsation and inclusion of nanoparticles in the pulsating flow case at Re = 200 and ϕ = 1 vol % led to enhance

Table 7 Thermal conductivity of different nanoparticles

Nanoparticles	Thermal conductivity/W m^{-1} K^{-1}	Ref.
Diamond	3300	[124]
MWCNT	2000–3000	[125]
SiC	490	[126]
Ag	429	[127]
Cu	398	[128]
Au	315	[129]
Al	247	[124]
Si	148	[124]
MgO	54.9	[129]
AlO_3	40.0	[130]
CuO	32.9	[124]
ZnO	29.0	[131]
TiO_2	8.4	[131]

heat transfer by 3%. Furthermore, heat transfer enhanced by 18.8% at Re = 200 and $\phi = 6$ vol%. Sakanova et al. [147] used three nanofluids to cool straight and wavy microchannels, including (Diamond–H_2O, CuO–H_2O, and SiO_2–H_2O). The authors found that wavy channels enhance heat transfer more than straight channels. Also, it is noted that the use of (Diamond–water) as the nanofluid coolant in a wavy channel enhanced heat transfer; moreover, when compared with straight channels, diamond–water nanofluid ranked the highest performance. Uysal et al. [148] studied the effect of utilizing (ZnO–ethylene glycol (EG)) nanofluid through rectangular microchannels on the heat characteristics numerically. Akbari et al.[149] investigated the effect of varying the height of the ribs in a straight microchannel on heat transfer performance. Al_2O_3 nanofluids with volume fractions ranging from 0.00 to 0.04 are used as a coolant inside a two-dimensional rectangular microchannel 2.5 mm long and 25 mm wide. The friction coefficient, rate of heat transfer, and average Nusselt number increased as the rib heights and nanoparticle volume fractions were increased. Modifying the solid volume fraction and rib height also significantly changes the temperature and dimensionless velocity along the flow's centerline in the ribbed regions, according to the simulation results. display previous literature studies on calculating the dynamic viscosity.

Sivakumar et al. [150] performed an experimental study to show the effect of nanofluids (Al_2O_3–H_2O and CuO–H_2O) on the forced convection heat transfer in a serpentine-shaped microchannel heat sink with a hydraulic diameter of 0.81 mm and volume fraction range (0–0.3%. The findings showed that when compared to distilled water and Al_2O_3–H_2O, CuO H_2O nanofluid has a higher heat transfer coefficient. Additionally, experimental results indicate that a higher volume fraction of nanoequal to (0.3%) will improve forced convective heat transfer.

Using the Eulerian and Lagrange methods, Nanofluids Al_2O_3 were used by Rostami and Abbassi [151] to evaluate heat transfer in a wavy microchannel. It is discovered that the wavy channel had a higher Nusselt number. While there was no discernible change in pressure drop, an increase in volume fraction resulted in a higher Nusselt number. Compared to a straight channel, heat augmentation, and drop of pressure were enhanced

Table 8 Previous studies related to thermal conductivity

References	Thermal conductivity of nanofluid	Conditions
Maxwell [130]	$\frac{k_{nf}}{k_{bf}} = \frac{k_p+2k_{bf}+2\phi(k_p-k_{bf})}{k_p+2k_{bf}-\phi(k_p-k_{bf})}$	Applicable for spherical sized particles
Hamilton–Crosser [131]	$\frac{k_{nf}}{k_{bf}} = \frac{k_p+(n-1)k_{bf}-(n-1)\phi(k_{bf}-k_p)}{k_p+(n-1)k_{bf}+\phi(k_{bf}-k_p)}$ $n = \frac{3}{\psi}$ n = empirical shape factor, dimensionless, ψ = sphericity, dimensionless, ψ = 1 for spherical	Shape factor taken in considerations
Pak and Cho [132]	$\frac{k_{nf}}{k_{bf}} = 1 + 7.47\phi$	Used for Al_2O_3 /Water nanofluid
Li and Peterson [133]	$\frac{k_{nf}}{k_{bf}} = 1 + 0.764481\phi + 0.01868867T - 0.46214175$	Used at temperature-dependent (27 °C ≤ T ≤ 36 °C) equation for Al_2O_3/H_2O
Xuan et al. [134]	$\frac{k_{nf}}{k_{bf}} = \frac{K_p+2K_{bf}-2(K_{bf}-K_p)\phi}{K_p+2K_{bf}+(K_{bf}-K_p)\phi}k_{bf} + \frac{\rho_p\phi C_p}{2k_{bf}}\sqrt{\frac{K_BT}{3\pi r_c\mu}}$ K_B = Boltzmann constant, rc = Apparent radius of clusters	Brownian motion taken in considerations
Xue [135]	$\frac{k_{nf}}{k_{bf}} = \frac{1-\phi+2\phi k_p/(k_{bf}-k_p)\ln\frac{k_p+kbf}{kbf}}{1-\phi+2\phi k_{bf}/(k_{bf}-k_p)\ln\frac{k_p+kbf}{kbf}}$	Used for CNT-based nanofluid
Yang et al. [136]	$\frac{k_{nf}}{k_{bf}} = \frac{k_p+2k_{bf}+2\phi(k_p-k_{bf})}{k_p+2k_{bf}-\phi(k_p-k_{bf})} + 157.5\phi C_f u_p^2 t$ where Cf = Heat capacity of the fluid per unit volume, u_p = Brownian velocity of the nanoparticles, t = Relaxation time	Brownian convection in the nanofluid taken in consideration

Table 9 Previous studies related to dynamic viscosity equations

References	Dynamic viscosity of nanofluid	Conditions
Einstein [137]	$\frac{\mu_{nf}}{\mu_{bf}} = 1 + 2,5\emptyset$	Predicted dynamic viscosity for low volume concentration of nanofluid, where ($\phi \leq 0.02$)
Brinkman [138]	$\frac{\mu_{nf}}{\mu_{bf}} = \frac{1}{(1-\emptyset)^{2.5}}$	Applicable up to volume concentration 4%
Abu-Nada [139]	$\mu_{nf} = -0.155 - \frac{19.582}{T} + 0.794\emptyset + \frac{2094.47}{T^2} - 0.192\emptyset^2 - 8.11\frac{\emptyset}{T} - 27463.\frac{863}{T^3} + 0.127\emptyset^3 + \frac{1.6044\emptyset^2}{T} + 2.1754\frac{\emptyset}{T^2}$	Used for Al_2O_3 with (40%) water and (60%) EG with temperature-dependent
Batchelor [140]	$\frac{\mu_{nf}}{\mu_{bf}} = 1 + 2,5\emptyset + 6.5\emptyset^2$	Brownian motion has been taken in consideration
Pak et al. [132]	$\frac{\mu_{nf}}{\mu_{bf}} = 1 + 39.11\emptyset + 533.9\emptyset^2$	Predicted dynamic viscosity for Al_2O_3/Water, TiO_2/Water nanofluid at room temperature
Nguyen et al. [43]	$\frac{\mu_{nf}}{\mu_{bf}} = 2.1275 - 0.0215T + 0.00027T^2)$	Used for temperature-dependent
Wang et al. [142]	$\frac{\mu_{nf}}{\mu_{bf}} = 1 + 7.3\emptyset + 123\emptyset^2$	Particle concentration taken in consideration

by 162.3 and 195.7%, respectively, when a wavy channel was used. Increases in pressure drops were observed to occur with the use of nanofluid. The ΔP by 2.4%, and the Nu increased by 11.6% for a volume factor of 0.02. Anbumeenakshi and Thansekhar, [152] used Al_2O_3 Nanofluids as the cooling fluid to indicate the performance of MCHS subjected to nonuniform heat flux. The experimental study employs three separate heaters of identical dimensions. A nonuniform heating condition is created by turning on any of the three heaters at the same time. For both uniform and nonuniform heat transfer, the average surface temperature dropped as volume concentration rose from 0.1 to 0.25%. Naphon et al. [153] studied experimentally using TiO_2 nanofluids on hydrothermal performance characteristics in the microchannel heat sink. This study uses three heat transfer enhancement techniques: microchannel heat sinks, jet impingement, and nanofluids. The obtained results demonstrated that at a nanofluid concentration of 0.015 vol%, suspending nanoparticles in the base fluid significantly increases convective heat transfer by 18.56%. Ali et al. [154] indicated experimentally and numerically the impact of various heat sink configurations and rates of working fluid flow using CuO–H_2O and Al_2O_3–H_2O with volumetric concentrations of 0.4% and 0.67%, respectively. Following the findings, Al_2O_3–H_2O nanofluid transferred heat faster than distilled water and CuO–H_2O nanofluid. The findings also showed that using nanofluids and increasing the flow rate decreased the base temperature. Heat transfer and hydrodynamic properties of a TiO_2–H_2O nanofluid used as a coolant through heat sinks with a wavy channel are investigated experimentally by Sajid et al. [155]. Performance of (TiO_2–H_2O) nanofluid at (0.006), (0.008), (0.01), and (0.012) vol% is compared to that of pure water in laminar flow with (25), (35), and (45) W heating capacity. The results demonstrate that, across all heat sinks, nanofluids outperformed distilled water regarding heat transfer characteristics.

Balaji et al. [156] studied the effect of using graphene nanoplatelets (GnP)/H_2O as nanofluid to improve thermal conductivity in a MCHS. Several heat transport metrics, including the coefficient of heat transfer, temperature drop, Nu, and ΔP, were investigated and found to be affected by both the mass flow rate (from 5 g s^{-1} to 30 g s^{-1}) and the concentration of GnP (from 0 to 0.2%). In experiments, using GnP–H_2O as nanofluids led to reduce the heat sink temperature by 10 °C, also the convective heat transfer coefficient increased by 71%, and increased the Nusselt number by 60%, respectively, In another side the pressure drop has been increased by 12% compared to water.

In a three-dimensional numerical study, Bazdar et al. [157] investigated heat transfer and turbulent flow in wavy MCHS with sinusoidal wavelengths. CuO–H_2O nanofluid has been used at Re numbers ranging from 3000 to 7500. The finding showed that by increasing Re to 7500, the HTP increased. While there is a little change in HTP approach to 3% at Re lower 7500 examined heat transfer and turbulent flow in a wavy microchannel with sinusoidal wavelengths in a three-dimensional numerical study. CuO–H_2O nanofluid was tested at Reynolds numbers from 3000 to 7500. The Nusselt number increased when the Reynolds number was greater than 7500 but did not change when it was less than 7500. Performance evaluation was worth 3%. Engineers and economists recommend nanofluids. Using a straight microchannel as a heat sink, Plant [158] utilized a variety of concentrations of Al_2O_3/H_2O nanofluid and porous media. Two and three channels have been used to assess different

Table 10 Previous studies related to using nanofluids

Ref	Sakanova et al. [147]			Wang et al. [145]	Ahmed et al. [144]	Hung [143]
Study type	Numerically			Experimentally	Numerically	Numerically
Microchannel geometry	Straight and wavy microchannels			The straight microchannel	Two-dimensional wavy channel	Double-layer microchannel
Re	99–232			Volume flow rate 200–1000 cm^3/min	100–800	600
Nanofluid	Diamond–H_2O	Cuo–H_2O	SiO_2–H_2O	Al_2O_3–H_2O	Cu–H_2O	Al_2O_3–H_2O
Volume fraction (%)	0–1			4	0–5	0.1–0.5 vol
Maximum enhancement in thermal performance	Heat transfer enhancement 22.93%			the best structure with the best nanofluid-cooled MCHS, led to best HTP, where it increased to 30%	Increasing of Nusselt number by 30	Increasing thermal performance by 26%

Ref	Anbumeena [152]	Rostami Abbassi [151]	Sivakumar et al. [150]		Akbari et al. [149]	Uysal et al. [148]
Study type	Experimentally	Numerically	Numerically		Numerically	Numerically
MCH geometry	Rectangular microchannel	Wavy microchannel	Serpentine-shaped microchannel		Rectangular microchannel	Rectangular microchannel
Re no	45–80	50–300	Re > 1308		10–100	10–100
Nanofluid type	Al_2O_3–H_2O	Al_2O_3–H_2O	CuO–H_2O	Al_2O_3–H_2O	Al_2O_3–H_2O	ZnO–ethylene glycol (EG)
Volume fracture %	0.1–0.25%	2%	0–0.3%	0–4%	0–4%	0–4%
Maximum enhancement in thermal performance	Effectiveness of performance are greater than unity in the range of operating conditions	The Nusselt number rose by 11.6%	Maximum heat transfer coefficient increased by 50% For Al_2O_3 and by 75% for CuO–H_2O		Maximum heat transfer coefficient increased by 11%	The increments in the convective heat transfer coefficient for 4% ZnO/EG nanofluid compared to pure EG are 19.33% and 16.89% at Re = 10 and Re = 100

Ref	Balaji et al. [156]	Sajid et al. [155]	Ali et al. [154]		Naphon et al. [153]
Study type	Experimentally	experimentally	Numerically and experimentally		Experimentally
MCH geometry	Straight MCHS	Wavy microchannel	Pin fin MCHS		Rectangular microchannel
Re No	Mass flow rate 5–30 g s^{-1}	500–1000	Flow rate 1–2 LPM		Mass flow rate 11 > g s^{-1}
Nanofluid type	Graphene(GnP–H_2O)	(TiO_2– H_2O)	Al_2O_3–H_2O	CuO–H_2O	TiO_2–H_2O
Volume fraction (%)	0–0.2 vol%	0.006–0.012) %	0.4–0.67%		1.5%
Maximum enhancement in thermal performance	71% and 60% increases in the convective heat coefficient (h) and Nu, respectively	Maximum enhancement in Nusselt number is noted as 40.57%	Heat transfer enhancement by 12%		Increasing of heat transfer coefficient by 18.56%

Ref	Alkasmoul et al. [160]				Heidarshenas et al. [159]	Plant and Saghir [158]	Bazdar et al. [157]
Case study	Experimentally and Numerically				Experimentally	Experimentally and Numerically	Numerically
MCH geometry	Straight microchannel				Cylindrical microchannel	Straight microchannels	Wavy microchannel
Re	Re > 2300				400–1200	Mass flow rate 2 g/min	3000–7500
Nanofluid type	CuO–H_2O	TiO_2–H_2O	SiO_2–H_2O	Al_2O_3–H_2O	Al_2O_3	Al_2O_3	CuO –H_2O
Volume fraction %	0–4	0–4	0–4	0–4	(20, 50, 80) nm (size of particle)	1–2%	0–3%

Table 10 (continued)

Ref	Alkasmoul et al. [160]	Heidarshenas et al. [159]	Plant and Saghir [158]	Bazdar et al. [157]
Maximum enhancement in thermal performance	The Nusselt number increases approximately by 20%	A rise of 21.9%, 21.1%, and 18.7% in Nu, respectively	Heat transfer enhancement by 24%	a-By increasing volume fraction from 0 to 3% at Reynolds number of 3000, the Nusselt number increases up to 84% b-By increasing volume fraction from 0 to 3% in at Reynolds number of 7500, the Nusselt number increases up to 87%

regions, with heat flow values ranging from 3.8328 to 10.3737 W cm^{-2}. Furthermore, the analyzed nanofluid was subjected to a range of flow rates. The results demonstrated a superior thermal enhancement of 24.5% for nanofluids with a 1% concentration compared to nanofluids with a 2% concentration. Heidarshenas et al.[159] conducted an experimental study to determine the impact of the various particle diameters of alumina nanoparticles Al_2O_3 (20, 50, 80, and 135 nm) on a forced convection coefficient of heat transfer in a cylindrical microchannel heat sink at different nanofluid flow rates. Their results demonstrated that increased particle size decreased the coefficient of heat transfer. At constant Reynolds number, the convective heat transfer coefficient increased for all particle sizes except 135 nm, where it decreased by 8.5%. For (20, 50, and 80 nm) a 21.9%, 21.1%, and 18.7% increase in Nu was observed. Alkasmoul et al. [160] presented a numerical study of the hydraulic and thermal performance of different nanofluids with different concentrations of nanoparticles in a microscopic heat sink for laminar flow. Based on previous work in cooling a microprocessor chip, a single rectangular microchannel is considered. The rectangular microchannel is silicon with a thermal conductivity of 130 W m^{-1} K^{-1}, and the working fluid is common nanoparticles—Al_2O_3, CuO, TiO_2, and SiO_2—in water because of their stability in the base. Utilizing nanofluid as a cooling liquid in an MCHS decreases thermal performance due to it cannot be sustained under low-temperature ranges

Table 11 Summary of previous studies related to using hyper nanofluid as coolant liquid

Ref	Pahlevaninejad et al. [171]	Bahiraei et al. [170]	Hussien et. al [169]	Kumar and Sarkar [168],	Nimmagadda [167]	Ho et al. [166]	S elvakuma [165]
Study type	Numerically	Numerically	Experimentally	Numerically	Numerically	Experimentally	Experimentally
Microchannel geometry	a wavy microchannel with rectangular obstacles	Two new microchannel	Microtube	Rectangular mini-channel	Rectangular microchannel	Rectangular mini-channel	Straight microchannel
Re	< 300	Inlet velocity 0.5–3 m s^{-1}	200–500	150–500	Re > 600	133–1515	Re > 2300
Hyper Nanofluid	Carboxymethyl cellulose/ Al_2O_3	Graphene-Ag	MWCNT/GNP	Al_2O_3–(MWCNTs)	Al_2O_3/silver/ H_2O	Al_2O_3/PCM/ H_2O	Al_2O_3/Cu/H_2O
Nanoparticle concentration	5 vol.%	0–0.1vol.%	0.075–0.125 mass%	0.01 vol. %	3 vol.%	0–10 mass%;	4 vol.%
Maximum enhancement in heat transfer (%)	Increasing Nusselt by 15%	The average heat transfer coefficient was increased by 58%	The average heat transfer coefficient was increased by 58%	The highest heat transfer coefficient enhancement was 15.6%	The convective heat transfer coefficient increased 126–148%	Convective heat transfer increased by 25%	The heat transfer coefficient increased by 24.35%

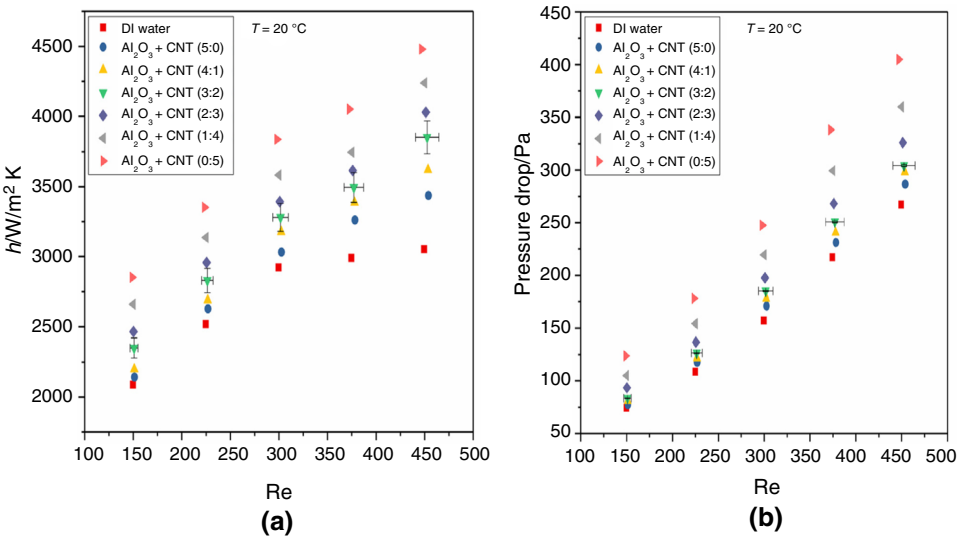

Fig. 16 **a** Variation of heat transfer coefficient with Re [182] **b** Variation of pressure drop with Re [182].

or because its pumping cost-effectiveness is inferior to that of water, according to the findings (Table 10).

Hybrid nanofluids in MCHS

Hybrid nanofluids could have greater thermal conductivity and heat transfer capacity than either mono- or conventional coolants. Numerous numerical and experimental studies have been devoted to the hydrothermal performance and exergy features of nanofluids in MCHS [161–164]. Combining hybrid nanofluids and microchannel heat sinks (MCHSs) has enhanced heat removal from heat flux electronic chips. In copper heat sinks, the convective heat transfer coefficient of an Al_2O_3/Cu hydrophilic hybrid nanofluid was analyzed by Selvakumar and Sures [165]. Their results showed that the hybrid nanofluid had better heat transfer than water. Convective heat transfer increased by 24.35% and pumping power by 12.61%. Ho et al. [166] examined Al_2O_3 hybrid nanofluid thermal performance in mini-channel heat sinks. Al_2O_3 nanofluids cool better than hybrid nanofluids based on Al_2O_3/microencapsulated phase change material. Nimmagadda [167] examined how an Al_2O_3/silver hybrid nanofluid affected MCHS heat transfer. The author concluded that the convective heat transfer coefficient increased by 126–148%. A similar study tested the heat transfer of an Al_2O_3/Ag binary hybrid nanocoolant in a rectangular microchannel. In addition, it was demonstrated that the coefficient of convective heat transfer increases as the volume fraction of the hybrid nanofluid increases.

Kumar and Sarkar [168] numerically examined a hybrid nanofluid's heat transfer and fluid flow characteristics based on Al_2O_3 multi-walled carbon nanotubes (MWCNTs) in mini-channel heat sinks under laminar flow conditions. The highest heat transfer coefficient enhancement was 15.6%, with no pressure drop. Hussien et al. [169] conducted an experimental study to assess the thermal performance and entropy generation characteristics of a microtube cooled with an MWCNT/GNP hybrid nanofluid with (Re) ranging from 200 to 500. In this case, the average coefficient of heat transfer was raised by 58%. In addition, increasing Re and vol% decreased thermal entropy production while increasing frictional entropy generation. Bahiraei et al. [170] conducted a numerical study of the thermohydraulic performance and entropy generation of various modified MCHSs cooled with a graphene–Ag hybrid nanofluid. Findings showed that surface temperatures dropped dramatically as volume fraction and inlet velocity increased. Increases in volume fraction and inlet velocity resulted in a significant boost in pumping power in a wavy microchannel. Pahlevaninejad et al. [171] examined the analysis of non-Newtonian nanofluid and rectangular ribs with five heights. As a working fluid, 0.5% carboxymethylcellulose and Al_2O_3 nanoparticles of varying volume friction and diameter were combined. In addition, ribs with different geometries are used as obstacles in the microchannels' middle wall. The Nusselt number increased as the proportion of nanofluid volume increased, and the greatest impediment produced the greatest friction factor. Souby et al. [172] explored a numerical study that used novel, reasonably priced binary/ternary hybrid nanofluids to assess how well MCHSs performed under the first and second laws. MgO/TiO_2 nanocomposite and CuO/MgO/TiO_2 nanocomposite are examples of binary and ternary hybrid nanofluids, respectively, that are based on water. When using hybrid nanofluids with high Re and vol. percent values, the convective heat transfer coefficient, pressure drop, and frictional entropy generation rate are all increased. Table 11 show a summary of studies related to using hybrid nanofluid.

Table 12 Summary of heat transfer enhancement and pressure drop in different shapes of MCHS

Heat transfer enhancing technique	MCHS type	Heat transfer enhancement	Pressure drop or friction coefficient	Conclusions
Corrugated	Wavy	Superior	Acceptable levels	Using MCHS with a hybrid technique can give a moderate pressure drop
	Zigzag	Superior	High levels	
	Convergent–divergent	Moderate	Moderate	Using at low Re No
flow disruption	Channel with reentrant cavities	Superior	Low	Used for a moderate range of Re to high, at low Re, reduce the pressure drop but low heat transfer enhancement
	Ribs	Good	High	The presence of ribs can interrupt the thermal boundary layer and create secondary flows and vortices, hence heat transfer enhancement
	Fins	The percentage of heat transfer depends on geometric configuration, generally, enhanced HTP with acceptable rang	Negligible when the fins are inclined	The presence of incline fins can make the fluid mix and interrupt the thermal boundary layer so enhance heat transfer with negligible pressure drop
	Dimples	Related by geometrical configuration of dimples	Related by geometrical configuration of dimples	A larger dimpled heat sink with a staggered dimple pattern results in a higher Nu and a higher friction factor
Fluid additives	Using nanofluid (hybrid or mono)	Enhance heat transfer with optimized value of, volume fraction of nanoparticle, nanoparticle size and design of MCHS	High pressure drop at high volume fraction of mono-nanofluid and moderate pressure drop when using hybrid nanofluid	Using the optimum design of MCHS with optimum value of volume fraction of hybrid nanofluid can give good heat transfer enhancement with low pressure drop

Effect of nanoparticle mixture ratios on HTP

Also, the HTP of hybrid nanofluids is highly sensitive to nanoparticle mixture ratios. The effect of the nanoparticle mixing ratio on the thermal performance of an Al_2O_3–TiO_2 hybrid nanofluid was investigated by Charab et al. [173]. It was determined that a ratio of 2:3 provided the greatest improvement in heat transfer (35.3%). The influence of the nanoparticle mixing ratio of an Al_2O_3-MWCNT hybrid nanofluid on the HTP of mini-channel heat sinks was experimentally examined by Kumar et al. [174]. Their research shows that a combined ratio of about 3:2 yields the highest hydrothermal performance. By doing experimental research on the conducted heat coefficient of Al_2O_3–SiO_2/Water hybrid nanofluids, Moldoveanu et al. [175] found that the hybrid nanofluid has superior thermal conductivity to alumina nanofluids. The experimental study of the thermal conductivity and viscosity of hybrid nanofluids with varying particle ratios was conducted by Hamid et al. [176]. Maximum thermal conductivity improvement of up to 16% was seen at a 1:4 ratio of TiO_2–SiO_2, while maximum dynamic viscosity was at a 5:5 ratio. Kumar 2019 [31] conducted an experimental investigation on the cooling equipment's heat transfer performance with the same set of nanoparticles and observed a maximum boost of 35.3% for a 2:3 ratio. The experimental investigation of the viscosity of Graphite–SiO_2 hybrid nanofluid by Dalklç et al. [177] at various volume concentrations and mass ratios revealed an increase in viscosity from 0.65–36.32% with an increase in volumetric concentration. Based on their research into the thermal conductivity and stability of Cu–Al_2O_3 hybrid nanofluids with varying mixing ratios, Siddiqui et al. [178] concluded that a mixing ratio of 5:5 was optimal for achieving desirable hydrothermal parameters. Thermophysical properties of (Al_2O_3–SiO_2/EG) nanofluid were studied by Zawawi et al. [179], who discovered that a mixing ratio of 60:40 resulted in the lowest property enhancement ratio. By testing several quantities of MWCNT (30 vol%) and Al_2O_3 (70 vol%) in 5 W50 oil (from 0.05 to 1%), Esfe et al. [180] determined that the greatest viscosity improvement was 24%. The ratios of nanoparticles in the mixture affect the heat transfer coefficient and the pressure drop, as shown in Fig. 11a, b. Selimefendigil et al. [181] reported that the heat transfer average rate can be increased with the addition of the nanoparticles but the ratios of nanoparticles volume fraction limited the rate of heat transfer enhancement.

Summary

Methods of heat transfer augmentation can be classified as passive and active techniques. Passive technique is the more technique that studied in the present work. The hydrothermal performance in MCHS restricted by high heat transfer and low pressure drop with low thermal resistance. So, Table 12 shows a summary to pressure drop which indicated friction coefficient.

Conclusions and recommendations

In this paper, an exhaustive review is presented of most configurations of the microchannel heat sink. Besides this, more than one type of nanofluid can be used as a cooling liquid. The main conclusions of the present work are as follows:

- With regards to corrugated MCHS the wavy MCHS outperforms the standard rectangular design when using water as a coolant. The heat resistance is lower in a wavy microchannel at a larger amplitude and a shorter wavelength.
- Wavy MCH with sinusoidal shape has superior HTP and low drop of pressure.
- Zigzag MCHS has good heat HTP but with high ΔP.
- With regards to flow disruptions, the MCHS with ribs can significantly enhance heat transfer due its ability to interrupt thermal boundary layer due to creating of secondary flow and vortices.
- The high drop in pressure can be induced at MCHS with rib, so the appropriate dimensions of ribs must be choose attentionally.
- The hybrid techniques (active with passive techniques) or (more than methods of passive) can improve the hydrothermal performance of MCHS.
- "Al_2O_3/H_2O," "CuO/H_2O," and "$TiO3/H_2O$" can be considered the most nanofluids used as coolant liquids for cooling electronic types of equipment.
- There are few papers dealing with the hyper nanofluid as coolant liquids.
- There are serious limitations in the study type of fluid flow such as turbulent or pulsating flow.
- The design of the microchannel is related to the application that is used to cool it, so the numerical analysis is not enough to study the thermal performance of the microchannel.
- Nanoparticle mixture ratio and size of nanoparticle effect on the hydrothermal performance of MCHS.
- Thermal conductivity increases with increasing concentration and temperature.
- The combination of using nanofluids has high HTP as cooling liquid with an optimized MCHS structure lead to efficient cooling of the MCHS.

Recommendations

- The current study demonstrated that the majority of existing research findings on using nanofluid as a cooling liquid in various MCHS concurred that using a nanofluid

with high thermal conductivity properties can improve heat dissipation. Fewer researchers are focused on the impact of other crucial nanofluid parameters like surface tension and contact angle, and stability of nanofluid on the cooling of MCHS, so in future research must give particular focus to how the characteristics of nanofluids, such as their surface tension and contact angle, affect MCHS cooling.

- Future studies must give attention to the combination between corrugated channels and
- flow disruptions technique.
- Effect of vibration induced in electronic system on MCHS performance.

References

1. Hetsroni G, Mosyak A, Segal Z, Ziskind G. A review of jet impingement cooling in microelectronics. Int J Heat Mass Transf. 2003;46:4595–610.
2. Ayub ZH, Mujtaba M, Zhang X, Han Z. Numerical and experimental investigation of microchannel heat sink for high concentration photovoltaic cells. Int J Hydrogen Energy. 2013;38:3279–88.
3. Kashani A, Mahjoob S. Compact heat exchangers: a review and future applications for a new generation of high-temperature solar receivers. Renew Sustain Energy Rev. 2012;16:3069–78.
4. Joshi Y, Kamath V. Performance analysis of microchannel heat exchanger for cooling of electric vehicle battery. Appl Therm Eng. 2017;112:737–49.
5. Leary M, Richardson RA, Mileham AR. A review of the development and performance of microchannel heat sinks for electronics cooling. Appl Therm Eng. 2006;26:1977–87.
6. Dixit T, Ghosh I. Review of micro-and mini-channel heat sinks and heat exchangers for single-phase fluids. Renew Sustain Energy Rev. 2015;41:1298–311.
7. Shi X, Li S, Mu Y, Yin B. Geometry parameters optimization for a microchannel heat sink with secondary flow channel. Int Commun Heat Mass Transf. 2019;104:89–100.
8. Ghani A, Sidik NAC, Mamat R, Najafi G, Ken TL, Asako Y, Japar WMAA. Heat transfer enhancement in microchannel heat sink using hybrid technique of ribs and secondary channels. Int J Heat Mass Transf. 2017;114:640–55.
9. Zargartalebi M, Azaiez J. Heat transfer analysis of nanofluid based microchannel heat sink. Int J Heat Mass Transf. 2018;127(Part B):1233–42.
10. Mohammed HA, Gunnasegaran P, Shuaib NH. Heat transfer in rectangular microchannels heat sink using nanofluids. Int Commun Heat Mass Transf. 2010;37(10):1496–503.
11. Ma DD, Xia GD, Li YF, Jia YT, Wang J. Effects of structural parameters on fluid flow and heat transfer characteristics in a microchannel with offset zigzag grooves in the sidewall. Int J Heat Mass Transf. 2016;101:427–35.
12. Sui Y, Teo CJ, Lee PS, Chew YT, Shu C. Fluid flow and heat transfer in wavy microchannels. Int J Heat Mass Transf. 2010;53(13–14):2760–72.
13. Li P, Zhang D, Xie Y, Xie G. Flow structure and heat transfer of non-Newtonian fluids in microchannel heat sinks with dimples and protrusions. Appl Therm Eng. 2016;94:50–8.
14. Li M, Chen X, Ruan X. Investigation of flow structure and heat transfer enhancement in rectangular channels with dimples and protrusions using large eddy simulation. Int J Therm Sci. 2020;149:106207. https://doi.org/10.1016/j.ijthermalsci.2019.106207.
15. Chai L, Xia G, Zhou M, Li J, Qi J. Optimum thermal design of interrupted microchannel heat sink with rectangular ribs in the transverse microchambers. Appl Therm Eng. 2013;51:880–9.
16. Chen Y, Fu P, Zhang C, et al. Numerical simulation of laminar heat transfer in microchannels with rough surfaces characterized by fractal Cantor structures. Int J Heat Fluid Flow. 2010;31:622–9.
17. Wang G, Qian N, Ding G. Heat transfer enhancement in microchannel heat sink with bidirectional rib. Int J Heat Mass Transf. 2019;136:597–609.
18. Wang R, Wang J, Lijin B, et al. Parameterization investigation on the microchannel heat sink with slant rectangular ribs by numerical simulation. Appl Therm Eng. 2018;133:428–38.
19. Chai L, Wang L, Bai X. Thermohydraulic performance of microchannel heat sinks with triangular ribs on sidewalls—part 1: local fluid flow and heat transfer characteristics. Int J Heat Mass Transf. 2018;127:1124–37. https://doi.org/10.1016/j.ijheatmasstransfer.2018.08.114.
20. Chai L, Wang L, Bai X. Thermohydraulic performance of microchannel heat sinks with triangular ribs on sidewalls—part 2: average fluid flow and heat transfer characteristics. Int J Heat Mass Transf. 2019;128:634–48.
21. Ma DD, Xia GD, Wang W, et al. Study on thermal performance of microchannel heat sinks with periodic jetting and throttling structures in sidewalls. Appl Therm Eng. 2019;158: 113764. https://doi.org/10.1016/j.applthermaleng.2019.113764.
22. Chai L, Xia GD, Wang HS. Parametric study on thermal and hydraulic characteristics of laminar flow in microchannel heat sink with fan-shaped ribs on sidewalls—part 1: heat transfer. Int J Heat Mass Transf. 2016;97:1069–80.
23. Chai L, Xia GD, Wang HS. Parametric study on thermal and hydraulic characteristics of laminar flow in microchannel heat sink with fan-shaped ribs on sidewalls—part 2: pressure drop. Int J Heat Mass Transf. 2016;97:1081–90.
24. Chai L, Xia GD, Wang HS. Parametric study on thermal and hydraulic characteristics of laminar flow in microchannel heat sink with fan-shaped ribs on sidewalls—part 3: performance evaluation. Int J Heat Mass Transf. 2016;97:1091–101.
25. Xia G, Ma D, Zhai Y, et al. Experimental and numerical study of fluid flow and heat transfer characteristics in microchannel heat sink with complex structure. Energy Convers Manag. 2015;105:848–57.
26. Xia G, Chai L, Zhou M, et al. Effects of structural parameters on fluid flow and heat transfer in a microchannel with aligned fan-shaped reentrant cavities. Int J Therm Sci. 2011;50:411–9.
27. Xia G, Chai L, Wang H, et al. Optimum thermal design of microchannel heat sink with triangular reentrant cavities. Appl Therm Eng. 2011;31:1208–19.
28. Chai L, Xia G, Zhou M, et al. Numerical simulation of fluid flow and heat transfer in a microchannel heat sink with offset fan-shaped reentrant cavities in sidewall. Int Commun Heat Mass Transf. 2011;38:577–84.
29. Ahmed HE, Ahmed MI. Optimum thermal design of triangular, trapezoidal and rectangular grooved microchannel heat sinks. Int Commun Heat Mass Transf. 2015;66:47–57.
30. Chai L, Xia G, Wang L, et al. Heat transfer enhancement in microchannel heat sinks with periodic expansion–constriction cross-sections. Int J Heat Mass Transf. 2013;62:741–51.
31. Kumar P. Numerical investigation of fluid flow and heat transfer in trapezoidal microchannel with groove structure. Int J Therm Sci. 2019;136:33–43. https://doi.org/10.1016/j.ijthermalsci.2018.10.006.

32. Bayrak E, Olcay AB, Serincan MF. Numerical investigation of the effects of geometric structure of microchannel heat sink on flow characteristics and heat transfer performance. Int J Therm Sci. 2019;135:589–600. https://doi.org/10.1016/j.ijthermalsci.2018.08.030.
33. Xia G, Zhai Y, Cui Z. Numerical investigation of thermal enhancement in a micro heat sink with fan-shaped reentrant cavities and internal ribs. Appl Therm Eng. 2013;58:52–60.
34. Li YF, Xia GD, Ma DD, et al. Characteristics of laminar flow and heat transfer in microchannel heat sink with triangular cavities and rectangular ribs. Int J Heat Mass Transf. 2016;98:17–28. https://doi.org/10.1016/j.ijheatmasstransfer.2016.03.022.
35. Zhai YL, Xia GD, Liu XF, et al. Heat transfer in the microchannels with fan-shaped reentrant cavities and different ribs based on field synergy principle and entropy generation analysis. Int J Heat Mass Transf. 2014;68:224–33. https://doi.org/10.1016/j.ijheatmasstransfer.2013.08.086.
36. Zhai YL, Xia GD, Liu XF, et al. Exergy analysis and performance evaluation of flow and heat transfer in different micro heat sinks with complex structure. Int J Heat Mass Transf. 2015;84:293–303. https://doi.org/10.1016/j.ijheatmasstransfer.2015.01.039.
37. Ghani IA, Kamaruzaman N, Sidik NAC. Heat transfer augmentation in a microchannel heat sink with sinusoidal cavities and rectangular ribs. Int J Heat Mass Transf. 2017;108:1969–81. https://doi.org/10.1016/j.ijheatmasstransfer.2017.01.046.
38. Go JS. Design of a microfin array heat sink using flow-induced vibration to enhance the heat transfer in the laminar flow regime. Sens Actuators A. 2003;105:201–10.
39. Krishnaveni T, Renganathan T, Picardo JR, et al. Numerical study of enhanced mixing in pressure-driven flows in microchannels using a spatially periodic electric field. Phys Rev E. 2017;96:033117.
40. Selimefendigil F, Ghachem K, Albalawi H, AlShammari BM, Labidi T, Kolsi L. Thermal and phase change process of nanofluid in a wavy PCM installed triangular elastic walled ventilated enclosure under magnetic field. Case Stud Therm Eng. 2023;10:103169.
41. Wang H, Chen Z, Gao J. Influence of geometric parameters on flow and heat transfer performance of micro-channel heat sinks. Appl Therm Eng. 2016;107:870–9. https://doi.org/10.1016/j.applthermaleng.2016.07.039.
42. Li J, Peterson GP. 3-Dimensional numerical optimization of silicon-based high performance parallel microchannel heat sink with liquid flow. Int J Heat Mass Transf. 2007;50:2895–904. https://doi.org/10.1016/j.ijheatmasstransfer.2007.01.019.
43. Kou H-S, Lee J-J, Chen C-W. Optimum thermal performance of microchannel heat sink by adjusting channel width and height. Int Commun Heat Mass Transf. 2008;35:577–82. https://doi.org/10.1016/j.icheatmasstransfer.2007.12.002.
44. Chein R, Chen J. Numerical study of the inlet/outlet arrangement effect on microchannel heat sink performance. Int J Therm Sci. 2009;48:1627–38. https://doi.org/10.1016/j.ijthermalsci.2008.12.019.
45. Mansoor MM, Wong K-C, Siddique M. Numerical investigation of fluid flow and heat transfer under high heat flux using rectangular micro-channels. Int Commun Heat Mass Transf. 2012;39:291–7.
46. Shkarah AJ, Sulaiman MYB, Ayob MRBH, et al. A 3D numerical study of heat transfer in a single-phase micro-channel heat sink using graphene, aluminum and silicon as substrates. Int Commun Heat Mass Transf. 2013;48:108–15.
47. Feng Z, Luo X, Guo F, et al. Numerical investigation on laminar flow and heat transfer in rectangular microchannel heat sink with wire coil inserts. Appl Therm Eng. 2017;116:597–609. https://doi.org/10.1016/j.applthermaleng.2017.01.091.
48. Yildizeli A, Cadirci S. Multi-objective optimization of a microchannel heat sink through genetic algorithm. Int J Heat Mass Transf. 2020;146:118847.
49. Xie G, Zhang F, Sundén B, Zhang W. Constructal design and thermal analysis of microchannel heat sinks with multistage bifurcations in single-phase liquid flow. Appl Therm Eng. 2014;62:791–802. https://doi.org/10.1016/j.applthermaleng.2013.10.042.
50. Leng C, Wang X-D, Wang T-H. An improved design of double-layered microchannel heat sink with truncated top channels. Appl Therm Eng. 2015;79:54–62. https://doi.org/10.1016/j.applthermaleng.2015.01.015.
51. Shen H, Wang C-C, Xie G. A parametric study on thermal performance of microchannel heat sinks with internally vertical bifurcations in laminar liquid flow. Int J Heat Mass Transf. 2018;117:487–97. https://doi.org/10.1016/j.ijheatmasstransfer.2017.10.025.
52. Ghorbani N, Targhi MZ, Heyhat MM, et al. Investigation of wavy microchannel ability on electronic devices cooling with the case study of choosing the most efficient microchannel pattern. Sci Rep. 2022. https://doi.org/10.1038/s41598-022-09859-6.
53. Sui Y, Teo CJ, Lee PS, et al. Fluid flow and heat transfer in wavy microchannels. Int J Heat Mass Transf. 2010;53:2760–72. https://doi.org/10.1016/j.ijheatmasstransfer.2010.02.022.
54. Sui Y, Lee PS, Teo CJ. An experimental study of flow friction and heat transfer in wavy microchannels with rectangular cross section. Int J Therm Sci. 2011;50:2473–82. https://doi.org/10.1016/j.ijthermalsci.2011.06.017.
55. Gong L, Kota K, Tao W, et al. Parametric numerical study of flow and heat transfer in microchannels with wavy walls. J Heat Transf. 2011. https://doi.org/10.1115/1.4003284.
56. Xie G, Liu J, Zhang W, et al. Analysis of flow and thermal performance of a water-cooled transversal wavy microchannel heat sink for chip cooling. J Electron Packag. 2012. https://doi.org/10.1115/1.4023035.
57. Yong JQ, Teo CJ. Mixing and heat transfer enhancement in microchannels containing converging-diverging passages. J Heat Transf. 2014. https://doi.org/10.1115/1.4026090.
58. Gong L, Lu H, Li H, et al. Parametric numerical study of the flow and heat transfer in a dimpled wavy microchannel. Heat Transf Res. 2016;47:105–18. https://doi.org/10.1615/Heattransres.2015010726.
59. Ghani IA. Heat transfer analysis in multi-configuration microchannel heat sink. [Doctoral Dissertation], University Teknologi Malaysia. 2018.
60. Kumar S, Sarkar M, Singh PK, et al. Study of thermal and hydraulic performance of air cooled minichannel heatsink with novel geometries. Int Commun Heat Mass Transf. 2019;103:31–42. https://doi.org/10.1016/j.icheatmasstransfer.2019.02.008.
61. Memon SA, Cheema TA, Kim GM, et al. Hydrothermal investigation of a microchannel heat sink using secondary flows in trapezoidal and parallel orientations. Energies. 2020;13:5616. https://doi.org/10.3390/en13215616.
62. Khan MZU, Younis MY, Akram N, et al. Investigation of heat transfer in wavy and dual wavy micro-channel heat sink using alumina nanoparticles. Case Stud Therm Eng. 2021;28:101515. https://doi.org/10.1016/j.csite.2021.101515.
63. Memon SA, Akhtar S, Cheema TA, et al. Investigation of the hydrothermal phenomena in a wavy microchannel with secondary flow passages through mid-wall inflection points. Appl Therm Eng. 2023;223:120010. https://doi.org/10.1016/j.applthermaleng.2023.120010.
64. Wang S-L, An D, Yang Y-R, et al. Heat transfer and flow characteristics in symmetric and parallel wavy microchannel heat sinks

with porous ribs. Int J Therm Sci. 2023;185:108080. https://doi.org/10.1016/j.ijthermalsci.2022.108080.
65. Ho CJ, Chang P-C, Yan W-M, et al. Efficacy of divergent minichannels on cooling performance of heat sinks with water-based MEPCM suspensions. Int J Therm Sci. 2018;130:333–46. https://doi.org/10.1016/j.ijthermalsci.2018.04.035.
66. Liu H, Li PW, Lew JV. CFD study on flow distribution uniformity in fuel distributors having multiple structural bifurcations of flow channels. Int J Hydrogen Energy. 2010;35:9186–98.
67. Kumaran RM, Kumaraguruparan G, Sornakumar T. Experimental and numerical studies of header design and inlet/outlet configurations on flow mal-distribution in parallel micro-channels. Appl Therm Eng. 2013;58:205–16.
68. Ghani IA, Sidik NAC, Kamaruzzaman N, Yahya WJ, Manhian O. The effect of manifold zone parameters on the hydrothermal performance of micro-channel Heat Sink: a review. Int J Heat Mass Transf. 2017;109:1143–61.
69. Vinodhan VL, Rajan KS. Computational analysis of new microchannel heat sink configurations. Energy Convers Manag. 2014;86:595–604.
70. Mohammed HA, Gunnasegaran P, Shuaib NH. Influence of channel shape on the thermal and hydraulic performance of microchannel heat sink. Int Commun Heat Mass Transf. 2011;38:474–80. https://doi.org/10.1016/j.icheatmasstransfer.2010.12.031.
71. Zheng Z, Fletcher DF, Haynes BS. Laminar heat transfer simulations for periodic zigzag semicircular channels: Chaotic advection and geometric effects. Int J Heat Mass Transf. 2013;62:391–401. https://doi.org/10.1016/j.ijheatmasstransfer.2013.02.073.
72. Ma DD, Xia GD, Wang J, Yang YC, Jia YT, Zong LX. An experimental study on the hydrothermal performance of microchannel heat sinks with 4-ports and offset zigzag channels. Energy Convers Manag. 2017;152:157–65.
73. Duangthongsuk W, Wongwises S. An experimental investigation on the heat transfer and pressure drop characteristics of nanofluid flowing in a microchannel heat sink with multiple zigzag flow channel structures. Exp Therm Fluid Sci. 2017;87:30–9. https://doi.org/10.1016/j.expthermflusci.2017.04.013.
74. Tang W, Sun LC, Liu HT, Du M. Improvements in performance of a self-similarity heat sink through structure modification. Heat Transf Eng. 2019. 1–19.
75. Alnaqi AA, Alsarraf J, Al-Rashed AAAA, Afrand M. Thermal-hydraulic analysis and irreversibility of the MWCNTs-SiO_2/EG-H_2O non-Newtonian hybrid nanofluids inside a zigzag microchannels heat sink. Int Commun Heat Mass Transf. 2021;122:105158. https://doi.org/10.1016/j.icheatmasstransfer.2021.105158.
76. Peng Y, Li Z, Li S, et al. The experimental study of the heat ransfer performance of a zigzag-serpentine microchannel heat sink. Int J Therm Sci. 2021;163:106831. https://doi.org/10.1016/j.ijthermalsci.2021.106831.
77. Dewan A, Srivastava P. A review of heat transfer enhancement through flow disruption in a microchannel. J Therm Sci. 2015;24:203–14.
78. Chai L, Wang L. Thermal-hydraulic performance of interrupted microchannel heat sinks with different rib geometries in transverse microchambers. Int J Therm Sci. 2018;127:201–12.
79. Chai L, Xia GD, Wang HS. Numerical study of laminar flow and heat transfer in a microchannel heat sink with offset ribs on sidewalls. Appl Therm Eng. 2016;92:32–41.
80. Khan AA, Kim S-M, Kim K-Y. Performance analysis of a microchannel heat sink with various rib configurations. J Thermophys Heat Transf. 2015;30(4):1–9.
81. Kumar P. Numerical investigation of fluid flow and heat transfer in a trapezoidal microchannel with groove structure. Int J Therm Sci. 2019;136:33–43.
82. Ahmad F, Cheema TA, Ur Rehman MM, Abbas A, Woo Park C. Thermal enhancement of microchannel heat sink using rib surface refinements. Numer Heat Transf Part A Appl. 2019;7:851–70. https://doi.org/10.1080/10407782.2019.1673104.
83. Paramanandam K, Srinivasan B. Heat transfer enhancement in microchannels using ribs and secondary flows. Int J Numer Meth Heat Fluid Flow. 2022;32:2299–319.
84. Zhang S, Ahmad F, Ali H, Ali S, Akhtar K, Ali N, Badran M. Computational study of hydrothermal performance of microchannel heat sink with trefoil shape ribs. IEEE Access. 2022;10:74412–24. https://doi.org/10.1109/ACCESS.2022.3190496.
85. Lori MS, Vafai K. Heat transfer and fluid flow analysis of microchannel heat sinks with periodic vertical porous ribs. Appl Therm Eng. 2022;205:118059.
86. Wang G, Chen T, Tian M, Ding G. Fluid and heat transfer characteristics of the microchannel heat sink with truncated rib on sidewall. Int J Heat Mass Tranf. 2020;148:119142.
87. Yao P, Zhai Y, Li Z, Shen X, Wang H. Thermal performance analysis of multi-objective optimized microchannels with triangular cavity and rib based on field synergy principle. Case Stud Therm Eng. 2021;25:100963.
88. Siu-Ho A, Qu W, Pfefferkorn F. Experimental study of pressure drop and heat transfer in a single-phase micropin-fin heat sink. J Electron Packag. 2007;129:479–87.
89. Liu M, Liu D, Xu S, Chen Y. Experimental study on liquid flow and heat transfer in micro square pin fin heat sink. Int J Heat Mass Transf. 2011;54:5602–11.
90. Sajedi R, Osanloo B, Talati F, Taghilou M. Splitter plate application on the circular and square pin fin heat sinks. Microelectron Reliab. 2016;62:91–101.
91. Yadav V, Baghel K, Kumar R, Kadam ST. Numerical investigation of heat transfer in extended surface microchannels. Int J Heat Mass Transf. 2016;93:612–22.
92. Yu X, Woodcock C, Plawsky J, Peles Y. An investigation of convective heat transfer in a microchannel with Piranha Pin Fin. Int J Heat Mass Tran. 2016;103:1125–32.
93. Yang D, Wang Y, Ding G, Jin Z, Zhao J, Wang G. Numerical and experimental analysis of the cooling performance of single-phase array microchannel heat sinks with different pin-fin configurations. Appl Therm Eng. 2017;112:1547–56. https://doi.org/10.1016/j.applthermaleng.2016.08.211.
94. Al-Asadi MT, Al-damook A, Wilson MCT. Assessment of vortex generator shapes and pin fin perforations for enhancing water-based heat sink performance. Int Commun Heat Mass Transf. 2018;91:1–10. https://doi.org/10.1016/j.icheatmasstransfer.2017.11.002.
95. Wang J, Yu K, Ye M, Wang E, Wang W, Sundén B. Effects of pin fins and vortex generators on thermal performance in a microchannel with Al_2O_3 nanofluids. Energy. 2022. https://doi.org/10.1016/j.energy.2021.122606.
96. Wang Y, Shin JH, Woodcock C, Yu X, Peles Y. Experimental and numerical study about local heat transfer in a microchannel with a pin fin. Int J Heat Mass Transf. 2018;121:534–46.
97. Prajapati YK. Influence of fin height on heat transfer and fluid flow characteristics of rectangular microchannel heat sink. Int J Heat Mass Transf. 2019;137:1041–52.
98. Kadam ST, Kumar R, Abiev R. Performance augmentation of single-phase heat transfer in the open-type microchannel heat sink. J Thermophys Heat Transf. 2019;33(2):416–24.
99. Bhandari P, Prajapati YK. Thermal performance of open microchannel heat sink with variable pin fin height. Int J Therm Sci. 2021. https://doi.org/10.1016/j.ijthermalsci.2020.106609.
100. Shah RK. LONDON, Alexander Louis. Laminar flow forced convection in ducts: a source book for compact heat exchanger analytical data. Academic press, 2014.

101. Qu W, Mudawar I. Experimental and numerical study of pressure drop and heat transfer in a single-phase micro-channel heat sink. Int J Heat Mass Transf. 2002;45:2549–65.
102. Pandey J, et al. Comparison of the parallel microchannel and Pin-Fin heat sinks: an experimental study. Mater Today Proc. 2022;56:845–50.
103. Lan J, Xie Y, Zhang D. Flow and heat transfer in microchannels with dimples and protrusions. J Heat Transf Transf ASME. 2012;134(2):021901.
104. Bi C, Tang GH, Tao WQ. Heat transfer enhancement in minichannel heat sinks with dimples and cylindrical grooves. Appl Therm Eng. 2013;55(1–2):121–32.
105. Li P, Zhang D, Xie Y. Heat transfer and flow analysis of Al_2O_3–water nanofluids in a microchannel with dimple and protrusion. Int J Heat Mass Transf. 2014;73(73):456–67.
106. Li P, Xie Y, Zhang D, Xie G. Heat transfer enhancement and entropy generation of nanofluids laminar convection in microchannels with flow control devices. Entropy. 2016;18(4):1.
107. Xu M, Lu H, Gong L, Chai JC, Duan X. Parametric numerical study of the flow and heat transfer in microchannel with dimples. Int Commun Heat Mass Trans. 2016;76:348–57.
108. Li P, Xie Y, Zhang D. Laminar flow and forced convective heat transfer of shear-thinning power-law fluids in dimpled and protruded microchannels. Int J Heat Mass Transf. 2016;99:372–82.
109. Huang X, Yang W, Ming T, Shen W, Yu X. Heat transfer enhancement on a microchannel heat sink with impinging jets and dimples. Int J Heat Mass Transf. 2017;112:113–24. https://doi.org/10.1016/j.ijheatmasstransfer.2017.04.078.
110. Gan T, Ming T, Fang W, Liu Y, Miao L, Ren K, Ahmadi MH. Heat transfer enhancement of a microchannel heat sink with the combination of impinging jets, dimples, and side outlets. J Therm Anal Calorim. 2020;141:45–56.
111. Gupta A, Kumar M, Patil AK. Enhanced heat transfer in plate-fin heat sink with dimples and protrusions. Heat Mass Trans. 2019;55(8):2247–60.
112. Okab AK, Hasan HM, Hamzah M, Egab K, Al-Manea A, Yusaf T. Analysis of heat transfer and fluid flow in a microchannel heat sink with sidewall dimples and fillet profile. Int J Thermofluids. 2022;15:100192. https://doi.org/10.1016/j.ijft.2022.100192.
113. Debbarma D, Pandey KM, Paul A. Performance enhancement of double-layer microchannel heat sink by employing dimples and protrusions on channel sidewalls. Math Probl Eng. 2022. https://doi.org/10.1155/2022/2923661.
114. Ali ARI, Salam B. A review on nanofluid: preparation, stability, thermophysical properties, heat transfer characteristics and application. SN Appl Sci. 2020;2(10):1636.
115. Selimefendigil F, Öztop HF. Comparative study on different cooling techniques for photovoltaic thermal management: Hollow fins, wavy channel and insertion of porous object with hybrid nanofluids. Appl Therm Eng. 2023;228:120458.
116. Sadeghi R, et al. Investigation of alumina nanofluid stability by UV–vis spectrum. Microfluid Nanofluid. 2015;18:1023–30.
117. Saini A, et al. Nanofluids: a review preparation, stability, properties and applications. Int J Eng Res Technol. 2016;5(07):11–6.
118. Sahooli M, Sabbaghi S. CuO nanofluids: the synthesis and investigation of stability and thermal conductivity. J Nanofluids. 2012;1(2):155–60.
119. Pak BC, Cho YI. Hydrodynamic and heat transfer study of dispersed fluids with submicron metallic oxide particles. Exp Heat Transf Int J. 1998;11(2):151–70.
120. Zhou L-P, et al. On the specific heat capacity of CuO nanofluid. Adv Mech Eng. 2010;2:172085.
121. Xuan Y, Roetzel W. Conceptions for heat transfer correlation of nanofluids. Int J Heat Mass Transf. 2000;43(19):3701–7.
122. Sarkar J. A critical review on convective heat transfer correlations of nanofluids. Renew Sustain Energy Rev. 2011;15:3271–7. https://doi.org/10.1016/j.rser.2011.04.025.
123. Hwang Y, Park HS, Lee JK, Jung WH. Thermal conductivity and lubrication characteristics of nanofluids. Curr Appl Phys. 2006;6:67–71.
124. Lee SW, Park SD, Kang S, et al. Investigation of viscosity and thermal conductivity of SiC nanofluids for heat transfer applications. Int J Heat Mass Transf. 2011;54:433–8.
125. Bobkov V, Fokin L, Petrov E, et al. Thermophysical properties of materials for nuclear engineering: a tutorial and collection of data. In: International atomic energy agency, Vienna, Austria (2018)
126. Chung DDL. Materials for thermal conduction. Appl Therm Eng. 2001;21:1593–605.
127. Hofmeister AM. Thermal diffusivity and thermal conductivity of single-crystal MgO and Al_2O_3 and related compounds as a function of temperature. Phys Chem Miner. 2014;41:361–71.
128. Shackelford JF, Alexander W. CRC materials science and engineering handbook. 2000. https://doi.org/10.1604/9780849326967.
129. Kim SH, Choi SR, Kim D. Thermal conductivity of metal oxide nano fluid: particle size dependence and effect of laser irradiation. J Heat Transf. 2007;129:298–307.
130. Maxwell JC. A treatise on electricity and magnetism. Dover Books on Physics Ser. 2003;1. https://doi.org/10.1604/9780486606361.
131. Hamilton RL, Crosser OK. Thermal conductivity of heterogenous two-component systems. IEC Fundam. 1962;1:187–91.
132. Pak BC, Cho YI. Hydrodynamic and heat transfer study of dispersed fluids with submicron metallic oxide particles. Exp Heat Transf Int J. 1998;11:151–70.
133. Li C, Peterson GP. Experimental investigation of temperature and volume fraction variations on the effective thermal conductivity of nanoparticles suspensions (nanofluids). J Appl Phys. 2006;99:084314.
134. Xuan Y, Li Q, Hu W. Aggregation structure and thermal conductivity of nanofuids. AIChE J. 2003;49:1038–43.
135. Xue QZ. Model for thermal conductivity of carbon nanotube-based composites. Phys B Condens Matter. 2005;368:302–7.
136. Yang B. Thermal conductivity equations based on Brownian motion in suspensions of nanoparticles (nanofluids). J Heat Transf. 2008;130:042408.
137. Einstein A. A new determination of molecular dimensions. Ann Phys. 1906;19:289–306.
138. Brinkman HC. The viscosity of concentrated suspensions and solution. J Chem Phys. 1952;20:571–81.
139. Abu-Nada E. Effects of variable viscosity and thermal conductivity of Al_2O_3–water nanofluid on heat transfer enhancement in natural convection. Int J Heat Fluid Flow. 2009;30:679–769.
140. Batchelor GK. The effect of Brownian motion on the bulk stress in a suspension of spherical particles. J Fluid Mech. 1977;83(1):97–117.
141. Nguyen CT, Desgranges F, Roy G, et al. Temperature and particle-size dependent viscosity data for water-based nanofluids–hysteresis phenomenon. Int J Heat Fluid Flow. 2007;28:1492–506.
142. Wang X, Xu X, Choi SUS. Thermal conductivity of nanoparticle-fuid mixture. J Thermophys heat Transf. 1999;13:474–80.
143. Hung TC, Yan WM. Enhancement of thermal performance in a double-layered microchannel heat sink with nanofluids. Int J Heat Mass Transf. 2012;55(11–12):3225–38. https://doi.org/10.1016/j.ijheatmasstransfer.2012.02.057.
144. Ahmed MA, Shuaib NH, Yusoff MZ. Numerical investigations on the heat transfer enhancement in a wavy channel using nanofluid. Int J Heat Mass Transf. 2012;55(21–22):5891–8. https://doi.org/10.1016/j.ijheatmasstransfer.2012.05.086.

145. Wang XD, An B, Lin L, Lee DJ. Inverse geometric optimization for the geometry of nanofluid-cooled microchannel heat sink. Appl Therm Eng. 2013;55(1–2):87–94. https://doi.org/10.1016/j.applthermaleng.2013.03.010.
146. Selimefendigil F, Öztop HF. Forced convection and thermal predictions of pulsating nanofluid flow over a backward facing step with a corrugated bottom wall. Int J Heat Mass Transf. 2017;1(110):231–47.
147. Sakanova A, Keian CC, Zhao J. Performance improvements of the microchannel heat sink using wavy channel and nanofluids. Int J Heat Mass Transf. 2015;89:59–74. https://doi.org/10.1016/j.ijheatmasstransfer.2015.05.033.
148. Uysal C, Arslan K, Kurt H. A numerical analysis of fluid flow and heat transfer characteristics of ZnO-Ethylene glycol nanofluid in rectangular microchannels. Strojniski Vestnik/J Mech Eng. 2016;62(10):603–13. https://doi.org/10.5545/sv-jme.2015.3170.
149. Akbari OA, Toghraie D, Karimipour A, Safaei MR, Goodarzi M, Alipour H, Dahari M. Investigation of rib's height effect on heat transfer and flow parameters of laminar water-Al2O3 nanofluid in a rib-microchannel. Appl Math Comput. 2016;290:135–53. https://doi.org/10.1016/j.amc.2016.05.053.
150. Sivakumar A, Alagumurthi N, Senthilvelan T. Experimental investigation of forced convective heat transfer performance in nanofluids of Al_2O_3/water and CuO/water in a serpentine shaped micro channel heat sink. Heat Mass Transf. 2015;52:1265–74.
151. Rostami J, Abbassi A. Conjugate heat transfer in a wavy microchannel using nanofluid by two-phase Eulerian–Lagrangian method. Adv Powder Technol. 2016;27:9–18.
152. Anbumeenakshi C, Thansekhar MR. On the effectiveness of a nanofluid cooled microchannel heat sink under non-uniform heating condition. Appl Therm Eng. 2017;113:1437–43.
153. Naphon P, Nakharintr L, Wiriyasart S. Continuous nanofluids jet impingement heat transfer and flow in a micro-channel heat sink. Int J Heat Mass Transf. 2018;126:924–32. https://doi.org/10.1016/j.ijheatmasstransfer.2018.05.101.
154. Ali AM, Shoukat AA, Tariq HA, et al. Header design optimization of mini-channel heat sinks using CuO–H_2O and Al_2O_3–H_2O nanofluids for thermal management. Arab J Sci Eng. 2019;44:10327–38. https://doi.org/10.1007/s13369-019-04022-2.
155. Sajid MU, Ali HM, Sufyan A, et al. Experimental investigation of TiO_2–water nanofluid flow and heat transfer inside wavy mini-channel heat sinks. J Therm Anal Calorim. 2019;137:1279–94. https://doi.org/10.1007/s10973-019-08043-9.
156. Balaji T, Selvam C, Lal DM, et al. Enhanced heat transport behavior of micro channel heat sink with graphene based nanofluids. Int Commun Heat Mass Transf. 2020;117:104716. https://doi.org/10.1016/j.icheatmasstransfer.2020.104716.
157. Bazdar H, Toghraie D, Pourfattah F, et al. Numerical investigation of turbulent flow and heat transfer of nanofluid inside a wavy microchannel with different wavelengths. J Therm Anal Calorim. 2019;139:2365–80. https://doi.org/10.1007/s10973-019-08637-3.
158. Plant RD, Saghir MZ. Numerical and experimental investigation of high concentration aqueous alumina nanofluids in a two and three channel heat exchanger. Int Jo Thermofluids. 2021;9:100055. https://doi.org/10.1016/j.ijft.2020.100055.
159. Heidarshenas A, Azizi Z, Peyghambarzadeh SM, et al. Experimental investigation of heat transfer enhancement using ionic liquid-Al2O3 hybrid nanofluid in a cylindrical microchannel heat sink. Appl Therm Eng. 2021;191:116879. https://doi.org/10.1016/j.applthermaleng.2021.116879.
160. Alkasmoul FS, Asaker M, Almogbel A, et al. Combined effect of thermal and hydraulic performance of different nanofluids on their cooling efficiency in microchannel heat sink. Case Stud Therm Eng. 2022;30:101776.
161. Saadoon ZH, et al. Improving the performance of mini-channel heat sink by using wavy channel and different types of nanofluids. Sci Rep. 2022;12(1):9402.
162. Babar H, Ali HM. Towards hybrid nanofluids: preparation, thermophysical properties, applications, and challenges. J Mol Liq. 2019;281:598–633.
163. Selimefendigil F, Öztop HF. Analysis of hybrid nanofluid and surface corrugation in the laminar convective flow through an encapsulated PCM filled vertical cylinder and POD-based modeling. Int J Heat Mass Transf. 2021;178:121623.
164. Saadoon ZH, Ali FH, Sheikholeslami M. Numerical investigation of heat transfer enhancement using (Fe_3O_4 and Ag-H_2O) nanofluids in (converge-diverge) mini-channel heat sinks. Mater Today Proc. 2023;80:2983.
165. Selvakumar P, Suresh S. Use of A_2O_3–Cu water hybrid nanofluid in an electronic heat sink. IEEE Trans Compon Packag Manuf Technol. 2012;2:1600–7.
166. Ho C-J, Chen W-C, Yan W-M. Correlations of heat transfer effectiveness in a minichannel heat sink with water-based suspensions of Al2O3 nanoparticles and/or MEPCM particles. Int J Heat Mass Transf. 2014;69:293–9.
167. Nimmagadda R, Venkatasubbaiah K. Conjugate heat tranfer analysis of micro-channel using novel hybrid nanofluids (Al_2O_3 + Ag/Water). Eur J Mech-B/Fluids. 2015;52:19–27.
168. Kumar V, Sarkar J. Two-phase numerical simulation of hybrid nanofluid heat transfer in minichannel heat sink and experimental validation. Int Commun Heat Mass Transf. 2018;91:239–47.
169. Hussien AA, Abdullah MZ, Yusop NM, Al-Kouz W, Mahmoudi E, Mehrali M. Heat transfer and entropy generation abilities of MWCNTs/GNPs hybrid nanofluids in microtubes. Entropy. 2019;21:480.
170. Bahiraei M, Heshmatian S. Thermal performance and second law characteristics of two new microchannel heat sinks operated with hybrid nanofluid containing graphene–silver nanoparticles. Energy Convers Manag. 2018;168:357–70.
171. Pahlevaninejad N, Rahimi M, Gorzin M. Thermal and hydrodynamic analysis of non-Newtonian nanofluid in wavy microchannel. J Therm Anal Calorim. 2020;143:811–25. https://doi.org/10.1007/s10973-019-09229-x.
172. Souby MM, Bargal MHS, Wang Y. Thermohydraulic performance improvement and entropy generation characteristics of a microchannel heat sink cooled with new hybrid nanofluids containing ternary/binary hybrid nanocomposites. Energy Sci Eng. 2021;9:2493–513. https://doi.org/10.1002/ese3.982.
173. Charab AA, Movahedirad S, Norouzbeigi R. Thermal conductivity of Al_2O_3 + TiO_2/water nanofluid: model development and experimental validation. Appl Therm Eng. 2017;119:42–51.
174. Kumar V, Sarkar J. Particle ratio optimization of Al_2O_3-MWCNT hybrid nanofluid in minichannel heat sink for best hydrothermal performance. Appl Therm Eng. 2020;165:114546.
175. Moldoveanu GM, Huminic G, Minea AA, et al. Experimental study on thermal conductivity of stabilized Al_2O_3 and SiO_2 nanofluids and their hybrid. Int J Heat Mass Transf. 2018;127:450–7.
176. Hamid KA, Azmi WH, Nabil MF, Mamat R, Sharma KV. Experimental investigation of thermal conductivity and dynamic viscosity on nanoparticle mixture ratios of TiO_2–SiO_2 nanofluids. Int J Heat Mass Transf. 2018;116:1143–52.
177. Dalkılıç AS, Açıkgöz Ö, Küçükyıldırım BO, et al. Experimental investigation on the viscosity characteristics of water based

SiO_2-graphite hybrid nanofluids. Int Commun Heat Mass Transf. 2018;97(30):38.
178. Siddiqui FR, Tso CY, Chan KC, et al. On trade-off for dispersion stability and thermal transport of Cu–Al_2O_3 hybrid nanofluid for various mixing ratios. Int J Heat Mass Transf. 2019;132:1200–16.
179. Zawawi NNM et al. Experimental investigation on stability and thermo-physical properties of Al_2O_3–SiO_2/PAG nanolubricants with different nanoparticle ratios. J Therm Anal Calorim. 2019;135:1243–55.
180. Esfe MH, Abad ATK, Fouladi M. Effect of suspending optimized ratio of nanoadditives MWCNT-Al_2O_3 on viscosity behavior of 5W50. J Mol Liq. 2019;285:572–85.
181. Selimefendigil F, ÖZTOP HF. Forced convection and thermal predictions of pulsating nanofluid flow over a backward facing step with a corrugated bottom wall. Int J Heat Mass Transf. 2017;110:231–47.